

We measured both the magnetization and the magnetoresistance in pulsed magnetic fields extending to 60 T and in static fields up to 20 T at very low temperatures down to 30 mK.³ Figure 1a shows an example of an induced voltage signal. The Fourier transformation of the data below 40 T (Figure 1b) displays a dHvA frequency of 575 T corresponding to the so-called α

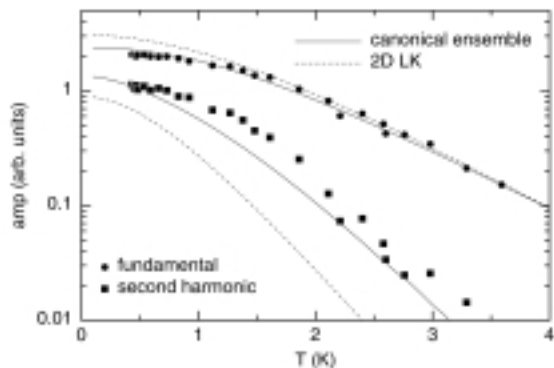


Figure 2. A comparison of the temperature dependences of the measured dHvA amplitudes with results using a numerical model (solid lines) and the LK theory.

pocket of the Fermi surface (FS) and the much larger frequency of 3875 T due to the breakdown β orbit. In many ways the oscillations below about 40 T reproduce the behavior seen in previous studies, with the exception of a β - α frequency which might be due to the oscillatory chemical potential in this 2D material. At higher magnetic fields the salt is taken deep into the magnetic-breakdown regime with a rich harmonic content of

the oscillations and finally a double-peak structure developing (Figure 1c). The latter structure is a result of well-resolved spin-split Landau levels in strong magnetic fields.

In contrast to the SdH effect, the oscillatory magnetization is a thermodynamic function of state, and is therefore able to probe the Fermi-liquid ground state directly. From the measured temperature dependences of the dHvA-oscillation amplitudes in pulsed field down to 0.4 K and in static fields down to 30 mK we obtain lower-than-expected effective masses when we fit the usual Lifshitz-Kosevich (LK) temperature reduction factor. At lower fields and higher temperatures the low-field value $m_c = 3.9 m_e$ ^[1] is extracted. While the sign of the apparent mass change is in agreement with our and previous SdH studies,² this change is much more acute in the SdH signal. Deviations from the LK behavior due to a fixed chemical potential can be calculated quantitatively by use of a numerical model.⁴ In the present case the effect of spin splitting is prominent and has to be taken into account properly. Figure 3 shows our experimental data for the fundamental and second harmonic of the dHvA amplitudes in comparison to the relative temperature dependences obtained from the numerical calculations by use of parameters extracted at low fields (solid lines) and with those of the LK theory (dashed lines). The numerical model describes the experimental dHvA data perfectly well.

¹ Heinecke, M., *et al.*, *Z. Phys. B*, **93**, 45 (1993).

² Balthes, E., *et al.*, *Z. Phys. B*, **99**, 163 (1996); *Synth. Metals* **94**, 3 (1998).

³ Harrison, N., *et al.*, *Phys. Rev. B*, **58**, 10248 (1998).

⁴ Harrison, N., *et al.*, *Phys. Rev. B*, **54**, 9977 (1996).

SEMICONDUCTORS

Large Magnetoresistance of Silver Selenide in a Pulsed Field

Betts, J.B., NHMFL/LANL

Balakirev, F.F., NHMFL/LANL

Boebinger, G.S., NHMFL/LANL

Rosenbaum, T.F., Univ. of Chicago, Physics

Saboungi, M.-L., Argonne National Laboratory

Schynders, H., ANL

Silver chalcogenides exhibit promising characteristics for possible use as magnetoresistive devices because of their large magnetoresistance (MR). Ag_2S , Ag_2Se and Ag_2Te are narrow-gap self-doped degenerate n-type semiconductors that show no appreciable MR. Previous investigations have shown that slight alterations in stoichiometry lead to a marked increase in magnetic response.^{1,2} Increases in resistivity up to 200% at 5.5 T have been observed. The MR is found to be unusually linear from a few mT up to several T.¹

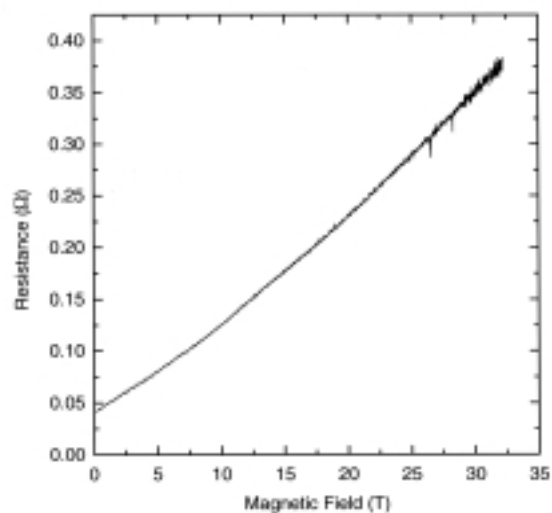


Figure 1. Magnetoresistance of $\text{Ag}_{2-\delta}\text{Se}$ at 1.5 K.

We investigated the magnetoresistive response in the off-stoichiometric Se-rich compound $\text{Ag}_{2-\delta}\text{Se}$ in pulsed magnetic fields up to 35 T. In this compound the electron density in the conduction band is largely determined by the stoichiometric

index δ . Samples with typical dimensions of 1-3 mm on a side and 1 mm thick were cut from long boules with a purity of 99.999%. These samples were then reduced in size to 2 mm x 1 mm x 1 mm to enable them to be mounted in the bore of the pulsed magnet. Resistance measurements were taken in a four probe geometry using the standard lock-in amplifier technique at 96 kHz. The field dependence of the resistance in the $\text{Ag}_{2-\delta}\text{Se}$ sample is presented in Figure 1. We find that the MR remains large with almost an order of magnitude increase in resistance from 0 T to 33 T with no signs of saturation. The low field linear regime seems to be limited to a magnetic field range below 5 T.

¹ Xu, R., *et al.*, Nature, **390**, 57 (1997).

² Chuprakov, I.S., *et al.*, Appl. Phys. Lett., **72**, 2165 (1998).

Theoretical Studies of Quantum Hall Matter

Bonesteel, N.E., NHMFL/FSU Physics

Melik-Alaverdian, V., Univ. of Rhode Island, Physics

Ortiz, G., LANL

(1) *Pairing of composite fermions at $\nu = 1/2$* . In this work the effect of statistical “gauge” fluctuations on the possible p-wave pairing of spin-polarized composite fermions was investigated.¹ It was found that these fluctuations are pair breaking in all angular momentum channels and so they tend to prevent any tendency towards pairing in the system. As the strength of the pairing interaction is increased, however, a first-order transition from compressible composite Fermi liquid to incompressible paired quantum Hall state can occur.

(2) *Numerical Studies of Skyrmions*. Numerical simulations have been used to study the effect of Landau level mixing on skyrmion excitations in the integer quantum Hall effect.² Both Landau level mixing and finite thickness of the two-dimensional electron gas were found to lower skyrmion excitation energies and favor skyrmions with fewer spin flips. The two effects do not work “coherently” however. When finite thickness is included the effect of Landau level mixing is strongly suppressed.

(3) *Quantum Monte Carlo on the Curved Surfaces*. A numerical algorithm for studying quantum Hall systems using Haldane’s spherical geometry, or quantum systems on any curved manifold, has been developed and tested against various test cases where analytic solutions are available.³

¹ Bonesteel, N.E., Phys. Rev. Lett., **82**, 984 (1999).

² Melik-Alaverdian, V. *et al.*, Phys. Rev. B, **82**, 984 (1999).

³ Melik-Alaverdian, V. *et al.*, Preprint.

Magneto-Optical Study of Interface Roughness in Type-II AlGaAs/AlAs Quantum Well Structures

Cheong, H.D., State Univ. of New York at Buffalo, Physics

Kioseoglou, G., SUNY at Buffalo, Physics

Petrou, A., SUNY at Buffalo, Physics

Dutta, M., U.S. Army Research Office, Research Triangle Park, NC

Pamulapati, J., U.S. Army Research Lab, Adelphi, MD

Wang, Y.J., NHMFL

Wei, X., NHMFL

Magnetoluminescence emission from MBE-grown AlGaAs/AlAs quantum wells is due to type-II recombinations of electrons populating the AlAs X-valleys and holes confined in the AlGaAs layers. The spectrum consists of an excitonic feature and strong LO-phonon replicas.¹ When a magnetic field is applied perpendicular to the structure’s layers a marked decrease in the photoluminescence (PL) intensity has been observed. This has been attributed to localization of electrons and holes on fluctuations on either side of the AlGaAs/AlAs interfaces. Carrier localization on the interfaces in a type-II system results in a reduction of the electron-hole wavefunction overlap and thus a decrease in the recombination probability.²

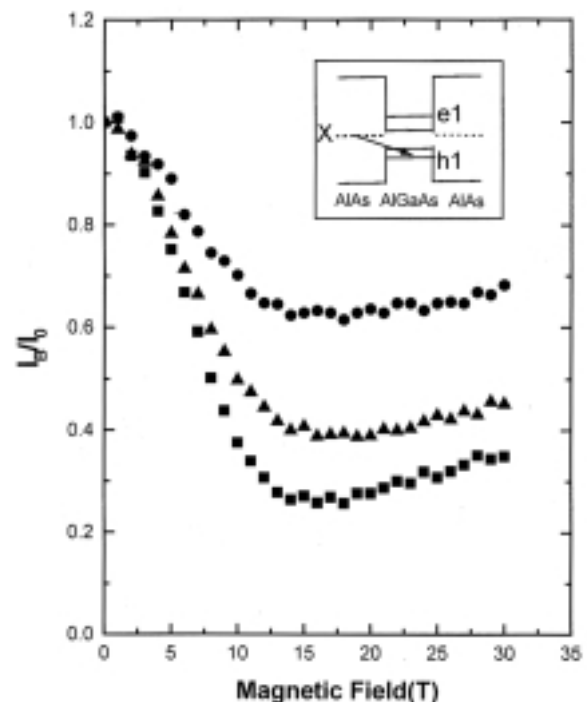


Figure 1. Intensity ratio I_B/I_0 plotted as a function of magnetic field, B. Here $I_B(I_0)$ is the intensity of the X_{h1} transition at B ($B=0$); squares: sample 1; triangles: sample 2; circles: sample 3.

We have modified the interface quality in a $(50\text{\AA}/100\text{\AA})_{20}$ AlGaAs/AlAs multiple quantum well structure by post-growth annealing at temperatures higher than the growth temperature of 620 °C. This study was carried out on three samples: Sample 1 was as grown and served as a reference; sample 2 was annealed for 1 minute at 670 °C; sample 3 was annealed for 1 minute at 710 °C. The results of the magneto-luminescence study are summarized in Figure 1 in which we plot the intensity ratio I_B/I_0 of the X_{h1} transition as function of applied field B . As the annealing temperature is increased, higher magnetic fields are required to produce the same PL intensity reduction. Using the magnetic fields for which I_B/I_0 extrapolates to zero, we determined the following magnetic lengths: (67 Å for sample 1; 57 Å for sample 2; 48 Å for sample 3). We interpret these results as indicating that the average size of the interface potential fluctuations decreases with increasing annealing temperature.

- ¹ Lee, S.T., *et al.*, Phys. Rev. B, **53**, 12912 (1996).
² Haetty, J., *et al.*, Phys. Rev. B, **56**, 12364 (1997).

Charged Excitons in Spin-Polarized 2D Electron Gases

Crooker, S.A., NHMFL/LANL
 Johnston-Halperin, E., Univ. of California at Santa Barbara, Physics
 Awschalom, D.D., Univ. of California at Santa Barbara, Physics
 Knobel, R., Pennsylvania State Univ., Physics
 Samarth, N., Pennsylvania State Univ., Physics

The low-temperature photoluminescence (PL) from a series of strongly magnetic n-type modulation-doped ZnSe/Zn(Cd,Mn)Se quantum wells in high magnetic fields (60 T) are investigated. These magnetic two-dimensional electron gases (2DEGs) exhibit a Zeeman spin splitting much larger than the cyclotron energy, leading to a highly spin-polarized 2DEG even at low magnetic fields, throughout the entire range of electron densities studied (5×10^{10} to $6.5 \times 10^{11} \text{ cm}^{-2}$). The giant Zeeman energy has a pronounced effect on the formation and energy of the singlet negatively charged exciton (X_s^- , which consists of two electrons with opposite spin bound to a single hole). Most notably, the energy separation of X_s^- from the neutral exciton is observed to follow the energy of the Fermi level, which in these magnetic 2DEGs may be tuned independently from the Landau levels through the temperature and applied field, as verified by numerical simulation. Further, the X_s^- is found to be rapidly suppressed at the $\nu=1$ quantum limit due to the unavailability of spin-up electrons.

Figure 1a shows the evolution of the PL spectra with applied field in a magnetic 2DEG having electron density $n_e = 1.24 \times 10^{11} \text{ cm}^{-2}$. The PL shifts rapidly to lower energy in the $\sigma+$ polarization, due to the large exchange-enhanced spin-splitting in this sample, and two clear PL peaks emerge which we assign to the neutral and charged exciton, X^0 and X_s^- . At $\nu=1$ the spectra collapse

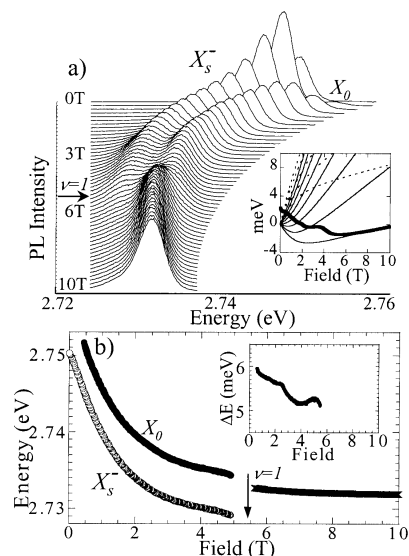


Figure 1. (a) PL spectra from a magnetic 2DEG to 10 T. Inset: The calculated spin-down (solid lines) and spin-up (dotted lines) Landau levels, and the Fermi energy. (b) Energies of the PL peaks, with the X_s^- - X^0 energy splitting shown in the inset.

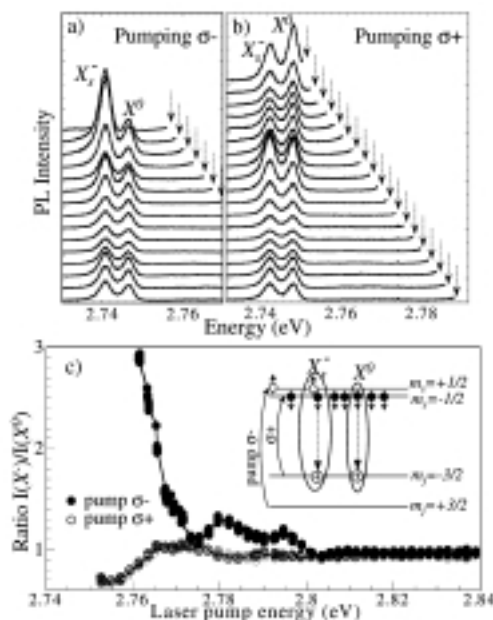


Figure 2. (a) pumping spin-up electrons enhances the X_s^- resonance, whereas (b) pumping spin-down electrons enhances the X^0 resonance. (c) The ratio of X_s^- and X^0 intensities, showing the $\sigma+$ and $\sigma-$ resonances more clearly.

and are replaced by a single peak at intermediate energy. The inset shows the calculated Landau levels and Fermi energy in this sample, indicating that the 2DEG is highly spin-polarized even in low magnetic fields. Figure 1b shows the energies of the PL features, along with the measured energy difference between the X^0 and X_s^- exciton (inset), which tracks the calculated Fermi energy.

The spin-singlet nature of the X_s^- exciton is verified in Figure 2, where we tune the energy and helicity of the pump laser.

Since the observed PL is entirely σ^+ polarized, it must arise from the recombination of a low-energy spin-down $m_s = -1/2$ electron with $m_j = -1/2$ hole in the valence band (see inset). If that $m_s = -1/2$ electron is part of an X_s^- complex, emission will occur at the X_s^- energy. When the 2DEG is highly spin-polarized, the probability of forming X_s^- is related to the number of spin-up ($m_s = +1/2$) electrons present in the system. By specifically injecting spin-up electrons at the σ^- resonance, we do indeed observe an enhancement of the X_s^- intensity, as shown in Figure 2a. In contrast, injecting spin-down electrons with σ^+ light can—and does—only favor the X^0 intensity (Figure 2b). The ratio of the intensities, $I(X_s^-)/I(X^0)$, is plotted in Figure 2c, where the effects of pumping on the σ^+ and σ^- resonances are more easily seen. Of related interest, no difference in this ratio is observed when exciting above the ZnSe barriers (2.8 eV) – evidence that the injected spin is scrambled when the electrons spill into the well from the barrier regions.

Field-Driven Annealing of the Magnetic Fluctuation Potential in Magnetic Semiconductor Quantum Wells

Crooker, S.A., NHMFL/LANL

Rickel, D.G., NHMFL/LANL

Lyo, K., Sandia National Laboratory

Samarth, N., Pennsylvania State Univ., Physics

Awschalom, D.D., Univ. of California at Santa Barbara, Physics

In contrast with nonmagnetic semiconductors, magnetic semiconductor alloys (e.g., $Zn_{1-x}Cd_xMn_ySe$) offer the unique possibility for tuning the magnetic disorder potential in a single sample through the application of magnetic field. The local conduction and valence band edges near a magnetic Mn^{2+} cation are closely tied to its spin orientation through the strong J_{sp-d} exchange interaction between the band electrons and holes and the localized d -electrons that comprise the $S=5/2$ Mn^{2+} spin. In a magnetic field, the local bandgap near a Mn^{2+} moment changes by $\pm 1/2(\alpha-\beta)[S_z]$ where $[S_z]$ is the expectation value of the Mn^{2+} spin and $(\alpha-\beta)$ is the J_{sp-d} exchange integral, usually of order 1 eV. At low temperatures, even modest fields ($H < 1T$) can dramatically shift—by hundreds of meV—the effective bandgap near the Mn^{2+} cations, directly changing the alloy disorder potential seen by a microscopic probe (such as an exciton) and serving as a clear and direct test of present theoretical models of alloy disorder broadening.

We observe direct evidence for a field-induced annealing of the magnetic fluctuation potential in single ZnSe/Zn(Cd,Mn)Se magnetic quantum wells.¹ A rapid reduction in the magnetic disorder, measured as a decrease in PL linewidth, occurs at low fields ($H < 5T$) as the isolated (paramagnetic) Mn^{2+} spins align, and then in stepwise fashion at $\sim 19 T$, $36 T$, and $53 T$ —precisely when antiferromagnetically-bound pairs of Mn^{2+}

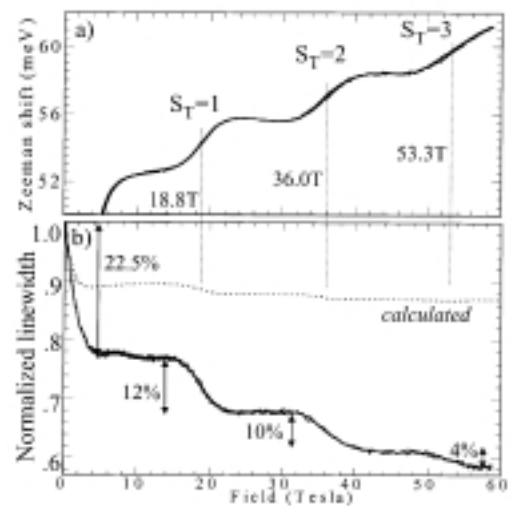


Figure 1. (a) The magnetization (\propto Zeeman shift) of the single magnetic quantum well, showing clear magnetization steps. (b) The corresponding linewidth of the PL, showing clear evidence of magnetic disorder annealing at the magnetization steps.

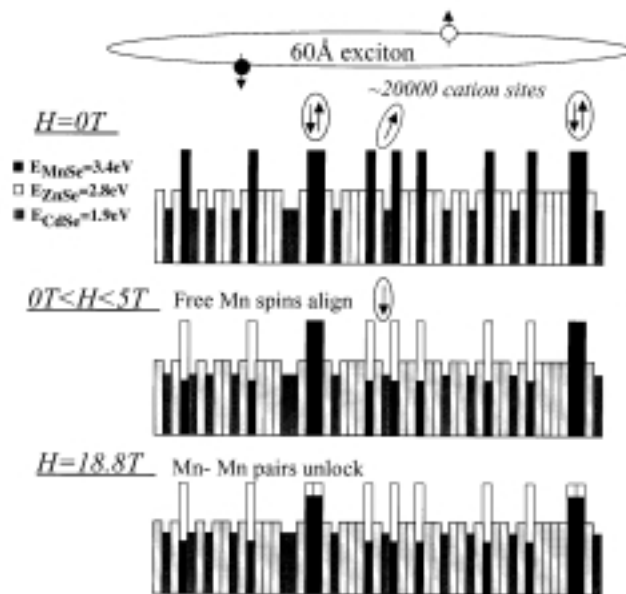


Figure 2. Schematic of the annealing process, whereby the local bandgap near Mn cations is reduced with field, thus reducing the overall fluctuation potential seen by excitons.

cations unlock. The magnitude of this stepwise linewidth annealing is over six times larger than predicted by present theories of disorder broadening in nonmagnetic semiconductor alloys, suggesting that revisions are required to include magnetic disorder.

Figures 1a and 1b show the measured magnetization (proportional to Zeeman energy shift) and PL linewidth in a

magnetic quantum well to 60 T. The linewidth clearly decreases at the magnetization steps, indicating that the magnetic disorder potential has smoothed. Schematically, Figure 2 shows the annealing process, wherein the local bandgap in the vicinity of the Mn cations is reduced with applied field, thereby reducing the overall root-mean-square fluctuations seen by the ensemble of ~ 60 Å excitons. Calculation of the rms fluctuation potential, based on existing theories developed for nonmagnetic semiconductors, reproduce the general shape of the observed linewidth annealing, but markedly underestimate the magnitude of the reduction.

¹ Crooker, S.A., *et al.*, Phys. Rev. B Rapid Comm., **60**, 2173 (1999).

Melting of the Electron Glass

Dobrosavljevic, V., NHMFL/FSU, Physics
Pastor, A.A., NHMFL

Understanding the basic physical processes determining whether a material is a conductor or an insulator continues to be a central theme of Condensed Matter Physics. The interplay of the electron-electron interactions and disorder is particularly evident deep on the insulating side of the metal-insulator transition. Here, both experimental and theoretical studies have demonstrated that they can lead to the formation of a soft "Coulomb gap", a phenomenon that is believed to be related to the glassy behavior of the electrons. Such glassy freezing has long been suspected to be of importance, but very recent work has suggested that it may even dominate the MIT behavior in certain low carrier density systems. The classic work of Efros and Shklovskii has clarified some basic aspects of this behavior, but a number of key questions remain. In particular: (1) What is the precise relation of this glassy behavior and the emergence of the Coulomb gap? (2) What should be the order parameter for the glass phase? (3) How should the glassy freezing affect the compressibility and the screening of the electron gas? (4) How do the quantum fluctuations (electron tunneling) melt this glass and influence the approach to the MIT?

In this project, we examine a simple model¹ for which all these questions can be rigorously answered in the limit of large coordination. When the interaction strength is large as compared to the Fermi energy, a low temperature glassy phase is identified through the emergence of an extensive number of metastable states, which in our formulation corresponds to a replica-symmetry breaking instability. The glassy phase is characterized by a pseudo-gap in the single particle density of states, reminiscent of the Coulomb gap of Efros and Shklovskii. Within our model, the universal form of the Coulomb gap proves to be a direct consequence of glassy freezing. Due to

ergodicity breaking, the "zero-field cooled" compressibility of this electron glass vanishes at $T=0$, consistent with absence of screening. Finally, we show that quantum fluctuations can melt this glass even at $T=0$, but that the relevant energy scale is set by the electronic mobility, and is therefore a nontrivial function of disorder. When the Fermi energy exceeds a critical value, the glassy phase is suppressed, and normal metallic behavior is recovered.

¹ Pastor, A.A., *et al.*, Phys. Rev. Lett., **83**, 4642 (1999)

Solitons on the Edge of Quantum Hall Systems

Dorsey, A.T., UF Physics
Wexler, C., UF Physics

Over the past decade a consistent theoretical picture of the low lying excitations of quantum Hall liquids (two dimensional electron systems in high magnetic fields) has emerged that is based on the physics of the edge of the droplet. Studies of these "edge states," however, have focussed on small amplitude, or linear, disturbances. Recently, we^{1,2} have shown that nonlinear effects may lead to "solitonic" edge states that propagate around the edge of the quantum Hall liquid without dispersion. These novel modes should be observable in time-of-flight measurements.

¹ Wexler, C. and Dorsey, A.T., Phys. Rev. Lett., **82**, 620 (1999).

² Wexler, C. and Dorsey, A.T., Phys. Rev. B, **60**, 10971 (1999).

High Magnetic Field Transport Near Landau Level Filling Factor $\nu = 1/2$ in a Thick Quantum Hall System

Du, R.R., Univ. of Utah, Physics
Zudov, M.A., Univ. of Utah, Physics
Simmons, J.A., Sandia National Laboratories
Reno, J.L., Sandia National Laboratories

We have studied the electronic transport near $\nu = 1/2$ in GaAs/AlGaAs quantum wells (QWs) in magnetic field B up to 33 T and at temperatures from 1.5 K to 50 mK. All QWs have an electron density $n = 3.6 \times 10^{11}/\text{cm}^2$ and a mobility $\mu = 3.5 \times 10^6 \text{ cm}^2/\text{Vs}$, but different well widths $d = 25, 30, 35, \text{ and } 40 \text{ nm}$, covering a range $d/\ell_B = 5$ to 8 for $\nu = 1/2$, where ℓ_B is the magnetic length.

For QWs having $d \geq 35 \text{ nm}$, a sharp magnetoresistance, R_{xx} , minimum centered at $\nu = 1/2$ ($B = 29.5 \text{ T}$) is observed, and is strongly temperature dependent. The R_{xx} exhibits weak

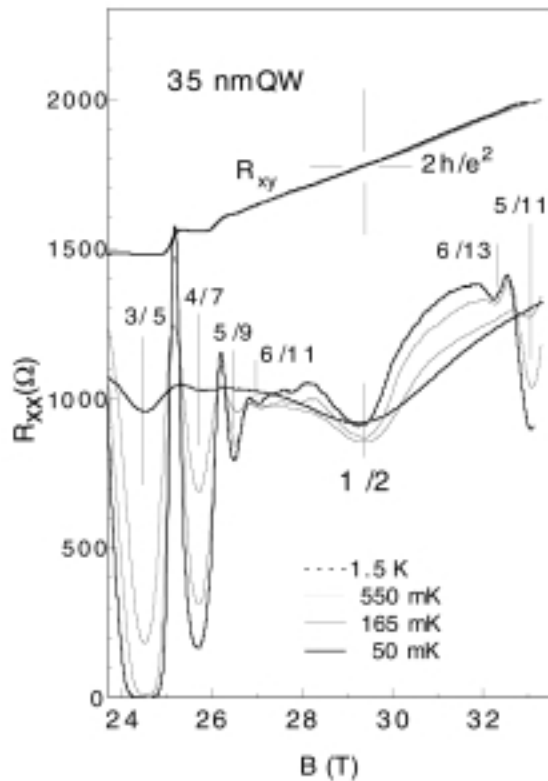


Figure 1. The magnetoresistance, R_{xx} , and Hall resistance, R_{xy} , near Landau level filling factor $\nu = 1/2$ measured in a 35 nm GaAs/AlGaAs quantum well sample at several temperatures in high magnetic field up to 33 T.

structures near $\nu = 1/2$, in addition to the sequence of the fractional quantum Hall states. Figure 1 shows the R_{xx} and the Hall resistance, R_{xy} , measured from a $d = 35$ nm QW at several temperatures.

These data deviate significantly from the characteristic composite Fermion transport¹ typical of single heterojunctions. Recent theoretical calculation² has shown an interesting possibility for p -wave pairing of composite fermions at $\nu = 1/2$, if the short-range part of the interaction is softened by increasing the thickness of the two-dimensional electron system. Experimentally, a fractional quantum Hall state at $\nu = 1/2$ in a wide single QW has been established, but it has been attributed to a two-component origin.³ Present high-density samples and high magnetic fields permit experiments in the range where the two-component state to Pfaffian state transition becomes accessible. Further experimental work at the NHMFL is planned to explore this regime.

Acknowledgement: This work is supported by NSF grant DMR-9705521.

¹ *Perspectives in Quantum Hall Effect - Novel Quantum Liquids in Low-Dimensional Semiconductor Structures*, ed. by S. Das Sarma and A. Pinczuk, Wiley and Sons, New York, 1997.
² Park, K., *et al.*, Phys. Rev. B, **58**, R10167 (1998).
³ See, e.g., Suen, Y.W., *et al.*, Phys. Rev. Lett., **68**, 1379 (1992).

Magnetotransport Study of Two-Dimensional Electron System in High Quality GaAs/AlGaAs Quantum Wells

Eom, J., Univ. of Chicago, Physics
 Kang, W., Univ. of Chicago, Physics
 Wegscheider, W., Schottky Institute

We have performed a magnetotransport study of the two-dimensional electron system (2DES) in high quality GaAs/AlGaAs quantum well (QW) samples at low temperatures and high magnetic fields. The experiment was performed on various QW samples with their well widths ranging from 175 to 250 Å and their electron density of $\sim 2 \times 10^{11} \text{ cm}^{-2}$. Typical mobilities of $\mu = \sim 4 \times 10^6 \text{ cm}^2/\text{Vs}$ are achieved in these samples at low temperatures. The magnetotransport in these narrow QW systems compares favorably with the 2DESs found in GaAs/AlGaAs heterostructures. In addition to the series of odd-numerator FQHE states, clearly defined magnetoresistance minima appear at even numerator fillings at $\nu = 5/2$ and $7/2$ below 100 mK. Further reduction in temperature enhances the even denominator FQHE states^{1,2} as well as the neighboring odd numerator FQHE states at $\nu = 7/3$ and $8/3$. These results, in comparison with those found in heterostructures, suggest that the z -direction confinement imposed by the finite well-thickness in the narrow QWs does not appreciably affect the even denominator FQHE states.³ Consequently, the role of finite thickness in the origin of even denominator FQHE states still remains an open question.⁴

¹ Willett, R.L., *et al.*, Phys. Rev. Lett., **59**, 1776 (1987).
² Eisenstein, J.P., *et al.*, Phys. Rev. Lett., **61**, 997 (1988).
³ Eom, J., *et al.*, unpublished.
⁴ Morf, R., Phys. Rev. Lett., **80**, 1505 (1998).

Novel Metallic Behavior in Two Dimensions [HRP]

Feng, X.G., NHMFL
 Popovic, D., NHMFL
 Washburn, S., Univ. of North Carolina at Chapel Hill, Physics
 Dobrosavljevic, V., NHMFL

Even though a recent discovery¹ of the metallic state and a metal-insulator transition (MIT) in two-dimensional (2D) systems has attracted a lot of attention, the origin of the metallic phase is still not understood. Until now, the 2D metallic phase has been characterized by an increase of conductivity σ as temperature $T \rightarrow 0$. Such a metallic behavior is suppressed both by magnetic field^{2,3} and by an arbitrarily small amount of scattering by electrons occupying some of the localized states associated with the upper subband⁴. Due to a large on-site Coulomb repulsion, such electrons may act as local magnetic moments. We have established that, in the presence of such

scattering, the 2D system exhibits a new and unexpected kind of metallic behavior, where σ decreases but does not go to zero (as expected for an insulator) when $T \rightarrow 0$.

The experiment was carried out on Si metal-oxide-semiconductor field-effect transistors (MOSFETs) in Corbino geometry with a width-to-length ratio of 20. The peak mobility was $\sim 1 \text{ m}^2/\text{Vs}$ at 4.2 K. With a bias of +1 V applied to the substrate to maximize the amount of scattering by local moments, an excellent fit to the data is obtained⁵ with $\sigma(n_s, T) = \sigma(n_s, T=0) + A(n_s)T^2$ over a wide range of n_s and over almost two decades in T ($0.045 < T < 2 \text{ K}$).

Figure 1 shows the zero-temperature conductivities $\sigma(n_s, T=0)$ as a function of $\delta_n = (n_s - n_c)/n_c$, the distance from the MIT (n_c - critical density), for two different samples. Finite values of $\sigma(n_s, T=0)$ mean that, in spite of the decrease of $\sigma(n_s, T)$ with decreasing T , the 2D system is in the metallic state. We find the power-law behavior

$$\sigma(n_s, T=0) \sim \delta_n^\mu \quad (\mu \approx 3),$$

as expected in the vicinity of a quantum critical point, such as the MIT. In addition, we have established⁵ that, in the vicinity of the MIT, the data can be described by a scaling form

$$\sigma(n_s, T) = \sigma_c(T) f(T/\delta_n^z)$$

(z and ν are the dynamical and correlation length exponents, respectively) with $\sigma_c \sim T^x$ ($x \approx 2.6$).

In contrast to the 2D conducting phase and the MIT discovered in Reference 1, the 2D metallic behavior studied here in the presence of a particular kind of disorder, has $d\sigma/dT > 0$, and the scaling form that describes the conductivity near the MIT includes a temperature dependent prefactor $\sigma_c(T)$, analogous to the MIT in three-dimensional (3D) systems. The observed $\sigma(n_s, T)$ is well established for 3D metals containing magnetic impurities, and is believed to result from the Kondo effect. In 2D, however, the existence of a metal with $d\sigma/dT > 0$ still awaits theoretical understanding, as it is inconsistent with the simple single-parameter scaling hypothesis⁶. Experiments involving a

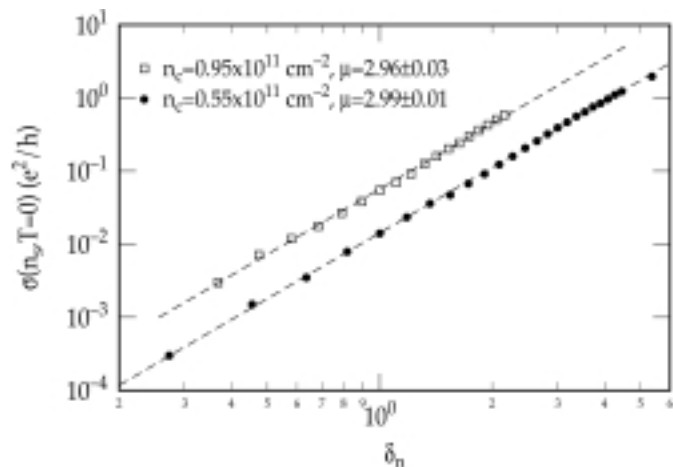


Figure 1. Zero-temperature conductivity vs. the distance from the MIT for samples 9 (squares) and 12 (dots). The dashed lines are fits with the slopes equal to the critical exponent μ .

wide range of magnetic fields are currently under way in order to gain further insight into the nature of this 2D conducting phase.

Acknowledgments: This work was supported by NSF Grant No. DMR-9796339, NHMFL, an NHMFL In-House Research Program Grant (D.P.), NSF Grant No. DMR-9974311 (V.D.), and Alfred P. Sloan Foundation (V.D.).

- 1 Kravchenko, S.V., *et al.*, Phys. Rev. B, **50**, 8039 (1994); Phys. Rev. B **51**, 7038 (1995).
- 2 Simonian, D., *et al.*, Phys. Rev. Lett., **79**, 2304 (1997).
- 3 Pudalov, V.M., *et al.*, JETP Lett., **65**, 932 (1997).
- 4 Feng, X.G., *et al.*, Phys. Rev. Lett., **83**, 368 (1999).
- 5 Feng, X.G., *et al.*, preprint cond-mat/9903236 (1999).
- 6 Dobrosavljevic, V., *et al.*, Phys. Rev. Lett., **79**, 455 (1997).

Photo-Darkening in Glassy As_2S_3

Hari, P., California State Univ. at Fresno, Physics
 Su, T., Univ. of Utah, Physics
 Taylor, P.C., Univ. of Utah, Physics
 Kuhns, P.L., NHMFL
 Moulton, W.G., NHMFL
 Sullivan, N.S., UF, Physics/NHMFL

Photo-darkening, or the shift of the optical absorption edge to smaller energies after excitation with light whose energy is near that of the optical band edge, has been studied in many chalcogenide glasses for many years.¹ Over the years many models have been proposed to account for this effect¹ but most of them fail because they do not pertain to essentially all of the atomic sites in the glass.

High field (up to 27 T) ^{75}As NMR measurements were performed using a 24.5 T DC magnet and a 30 T DC magnet. The pulsed NMR spectrometer was operated at about 125 MHz, a frequency that corresponds to a Zeeman field of approximately 17 T for ^{75}As . All NMR measurements were performed at 77 K. Details are available elsewhere.^{2,3} Photo-darkening was accomplished by irradiation of the samples at 300 K in air for approximately 230 hours. The irradiation source was an Ar^+ ion laser operating at 514.5 nm with about 170 mW/cm² at the sample. Annealing of the photo-darkening was accomplished by heating the sample in a furnace at 230 °C for 1.75 hours. Samples of glassy As_2S_3 were made by cutting and polishing bulk cylinders of approximately 2 cm diameter to a thickness of approximately 200 μm . At this thickness saturated photo-darkening occurs only in the first few microns of the sample, but some photo-darkening extends throughout the film.⁴

The high field NMR line shape at 77 K for ^{75}As in glassy As_2S_3 is shown in Figure 1. The solid circles are the experimental measurements and the solid line is a fit to the data to be described in the next section. The error in the data is represented by the scatter in the data points and is approximately $\pm 1\%$ of the maximum. The most distinctive features in this line shape,

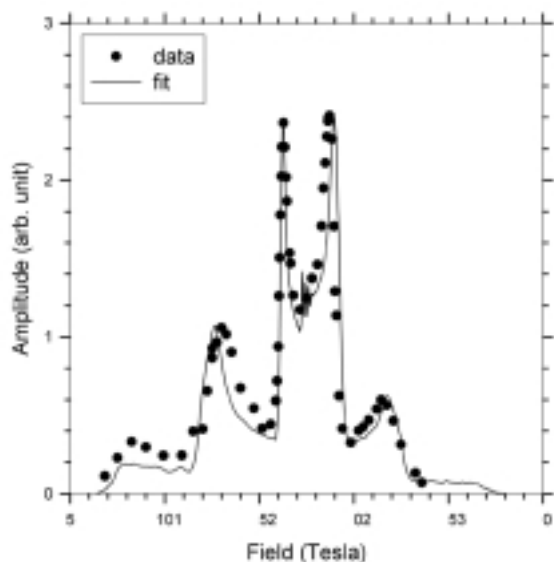


Figure 1. ^{75}As high field NMR absorption at 77 K in glassy As_2S_3 . Filled circles are experimental data and solid lines are theoretical fits as explained in the text. Experimental error in the data is $\pm 1\%$ of the maximum intensity.

the two peaks, or divergences, near 16 and 19 T are shown in Fig. 1. These two features are the most sensitive to small changes in asymmetry. The high field NMR line shape at 77 K for ^{75}As in irradiated glassy As_2S_3 is shown in Figure 2.

At first glance the spectrum in Fig. 2 looks very similar to the one before photo-darkening shown in Fig. 1. There is a difference, however, in the relative heights of the two divergences in Figs. 1 and 2. In Fig. 1 the low-field peak is smaller than the high-field peak while in Fig. 2 this trend is

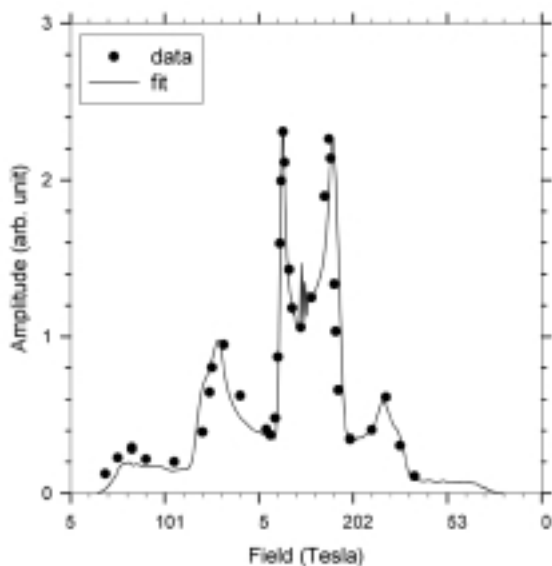


Figure 2. ^{75}As high field NMR absorption at 77 K in glassy As_2S_3 after irradiation at 300 K with light of wavelength 514.5 nm for 230 hours at 170 mW/cm^2 intensity on the sample. Filled circles are experimental data and solid lines are theoretical fits as explained in text. Experimental error in the data is $\pm 1\%$ of the maximum intensity.

reversed. The spectra were fit using a computer simulation that calculated the power pattern taking the quadrupole interaction as a second order perturbation on the Zeeman interaction.^{2,3} A distribution of quadrupolar coupling constants was obtained from the measured NQR line shape.^{2,3} In the fits displayed in Figs. 1 and 2 every e^2Qq/h was assumed to have the same η . The curve in Fig. 1 was calculated for $\eta = 0.09$ and that in Fig. 2 for $\eta = 0.12$. Fits were calculated for different η 's, and the error in both cases is estimated to be ± 0.1 . A symmetric, Gaussian distribution in η about $\eta = 0.09$ does not reproduce the spectrum in Fig. 2 no matter what the width. A symmetric, Gaussian distribution in η about $\eta = 0.12$ fits the spectrum in Fig. 2 within experimental error provided that the Gaussian width is less than about ± 0.1 . From these results we conclude that the average asymmetry of the As pyramidal sites increases on photo-darkening, and that photo-darkening is not explained by an increase in the width of the distribution of asymmetries at the As sites that keeps the average asymmetry constant.

- 1 Strom, U., *et al.*, J. Phys. Soc. Japan, **49**, Suppl. A, 1155 (1980).
- 2 Hari, P., *et al.*, Solid State Commun., **104**, 669 (1997).
- 3 Hari, P., *et al.*, Non-Cryst. Solids, **227-230**, 770 (1998).
- 4 Ducharme., *et al.*, Phys. Rev. B, **41**, 12250 (1990).

Spin Spectroscopy of CdSe Quantum Dots in High Magnetic Fields

Johnston-Halperin, E., Univ. of California at Santa Barbara, Physics
 Awschalom, D.D., UC Santa Barbara, Physics
 Crooker, S.A., NHMFL/LANL
 Peng, X., UC Berkeley, Chemistry
 Alivisatos, P.A., UC Berkeley, Chemistry

Chemically-synthesized CdSe quantum dots (QDs), provide an excellent system for investigating the physics of quantum confinement. The QDs are synthesized as free particles and placed in a non-interacting polymer matrix, minimizing inter-QD interactions that may complicate the interpretation of spectra. Photoluminescence spectroscopy allows the investigation of the quantum-confined electronic energy states without introducing extrinsic coupling. This spectroscopy is performed in high magnetic fields, giving access to an unusual regime where magnetic confinement and spin-dependent energies are comparable to the Coulomb interaction and quantum confinement effects.

Polarization-resolved photoluminescence (PL) of chemically synthesized CdSe QDs 40 to 80 Å in diameter has been performed at the NHMFL-Los Alamos in both the 40 and 60 T long-pulse (LP) magnets with temperatures $T = 1.2 - 50$ K. Polarization resolution was achieved by placing polarizing optics within the cryostat and alternating the field direction of the magnet (the 40 T LP magnet was retrofitted with field-reversing capability expressly for the purposes of this measurement). The excitonic luminescence was detected using a 0.3 m spectrometer with a fast back-thinned CCD at the output capable of collecting a spectrum every 1.5 ms, corresponding

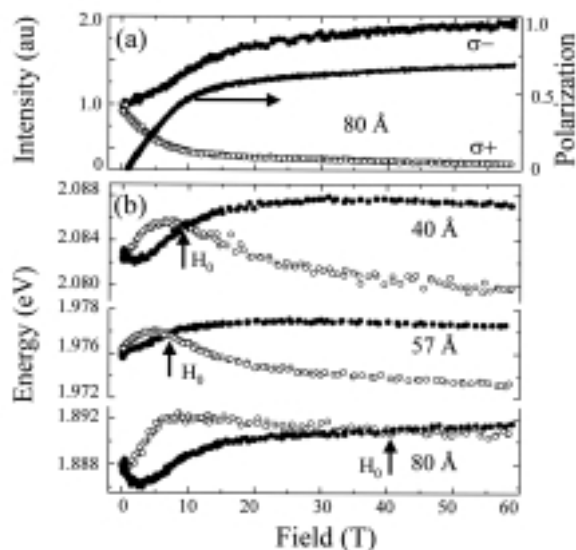


Figure 1. Energy, intensity, and polarization as determined by Gaussian fits to spectra for σ^+ (filled circles) and σ^- (open circles) polarized luminescence from 40, 57, and 80 Å QDs. (a) Intensity and polarization of 80 Å QDs at 1.2 K, qualitatively similar for all QDs studied. (b) Energy as a function of field at 1.2 K for 40 and 80 Å QDs, and 1.45 K for 57 Å QDs. Arrows indicate the crossing field H_0 . Additional data from the 57 Å QDs at 1.2 K up to 30 T shows no change from the 1.45 K behavior.

to a field variation of < 0.1 tesla/spectra and allowing the collection of an entire field dependence for each magnet shot. These spectra were then fit to a Gaussian lineshape to determine energy and intensity and analyzed as a function of applied magnetic field, revealing surprising behavior. Figure 1 (a) shows PL intensity versus magnetic field for the 80 Å diameter QDs, representative for all sizes studied. The intensities of the two polarization states behave qualitatively as expected for a thermal distribution of carriers between two Zeeman split energy levels. As can be seen in Figure 1 (b), however, the observed luminescence energies do not exhibit Zeeman behavior over a range of QD diameters. The energies of the two polarization states show level crossings at a QD diameter-dependent field, and at high fields exhibit the opposite relationship between energy and intensity that one would predict for a thermodynamic distribution of carriers.

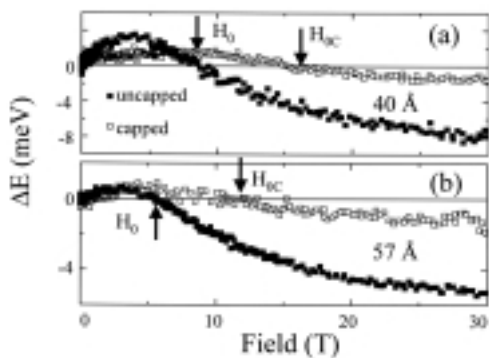


Figure 2. Energy splitting of capped and uncapped QDs for (a) 40 Å and (b) 57 Å diameter cores. Arrows indicate crossing fields H_0 and H_{0c} for uncapped and capped QDs respectively.

Some insight into this phenomenon can be gained by performing similar measurements on CdSe QDs capped with several monolayers of higher band gap CdS. This layer isolates the photoexcited carriers from the surface of the QDs. Figures 2 (a) and (b) show a comparison of the polarization energy difference (the difference between the energies of the σ^+ and σ^- polarizations of the luminescence) between two sample series consisting of identical CdSe cores both with and without the CdS capping layer. There are two effects present in these systems. The first, not shown, is a red shift in the zero field luminescence energy upon capping due to decreased confinement energy. This is due to carrier wavefunction leakage into the capping layer. The second, which can be seen in Figure 2, is a variation in the field dependent level crossing. Note that this variation is not due to a decrease in the confinement energy. If that were the case, one would expect the crossing point of the 40 Å capped QDs to be intermediate between that of the 40 Å uncapped and 57 Å uncapped QDs. It is possible that interactions with the surface states of the QDs are responsible for the differences in the observed crossings, which implies that this behavior is due to an interaction between bulk and surface states.

Techniques for Time and Spin Resolved Photoluminescence Studies of CdSe Quantum Dots in High Magnetic Fields

IHRP

Johnston-Halperin, E., Univ. of California at Santa Barbara, Physics

Awschalom, D.D., UC Santa Barbara, Physics

Crooker, S.A., NHMFL/LANL

Rickel, D., NHMFL/LANL

Peng, X., UC Berkeley, Chemistry

Alivisatos, P.A., UC Berkeley, Chemistry

Time-resolved spectroscopy is a powerful tool for exploring the dynamics of photo-excited carriers in a variety of systems. The addition of polarization resolution allows direct examination of carrier spin dynamics due to the selective coupling of circular polarizations of the luminescence to specific spin states through conservation of angular momentum. When performed in high magnetic fields, this technique can provide insight into carrier spin dynamics in a regime where spin dependent energies play a role in the physics comparable to Coulomb interactions and crystal symmetry considerations. Here we develop the capability to investigate exciton spin dynamics of CdSe quantum dots (QDs) at temperatures from 1.2 to 50 K and in fields up to 20 T through time-resolved photoluminescence (PL) studies with a time resolution of ~ 100 ps.

Time- and energy-resolved excitonic luminescence from CdSe QDs is obtained using the technique of time correlated single photon counting. Optical excitation is derived from the frequency doubled output of a mode locked Ti:Sapphire laser with a pulse length of ~ 100 fs, where the repetition rate of the excitation can be varied from 150 kHz to 76 MHz using an electro-optic pulse picker. Light is coupled to the

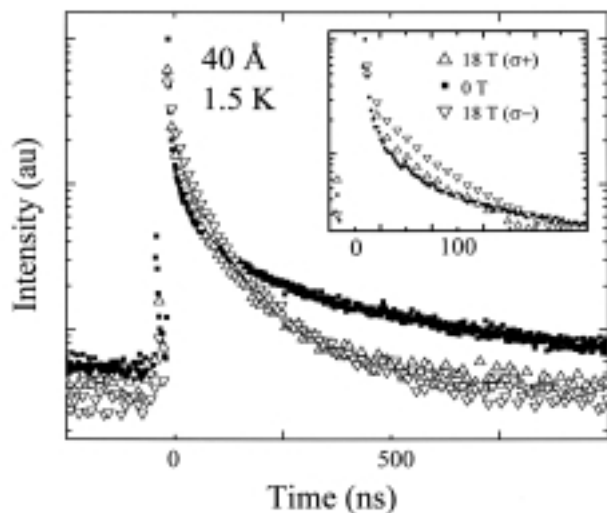


Figure 1. Photoluminescence decays for 40 Å diameter CdSe QDs at a temperature of 1.5 K for zero field (filled squares) and both σ^+ (open up triangles) and σ^- (open down triangles) polarizations at a field of 18 T. The inset shows the same data on a finer scale to highlight the deviation of the σ^- polarization at short time delays.

sample via an optical fiber and the collected luminescence is spectrally resolved by a monochromator with a multichannel-plate photomultiplier tube. Polarization resolution is obtained by placing polarizing optics in the cryostat between the sample and the collection fiber. The intrinsic system response is ~ 20 ps, but the measurements are limited to a resolution of ~ 100 ps due to modal dispersion in the multimode fiber.

Figure 1 displays the time- and polarization-resolved luminescence at zero field and 18 T, normalized to peak intensity, for 40 Å diameter QDs. The data are shown on a semi-log plot and are clearly not single or double exponential decays. There is a qualitative difference between the decays for the σ^+ and σ^- polarizations, indicating distinct recombination pathways. Further interesting behavior is revealed when the data are examined at fixed field as a function of temperature, as can be seen in Figure 2 for 40 Å diameter QDs at zero field and

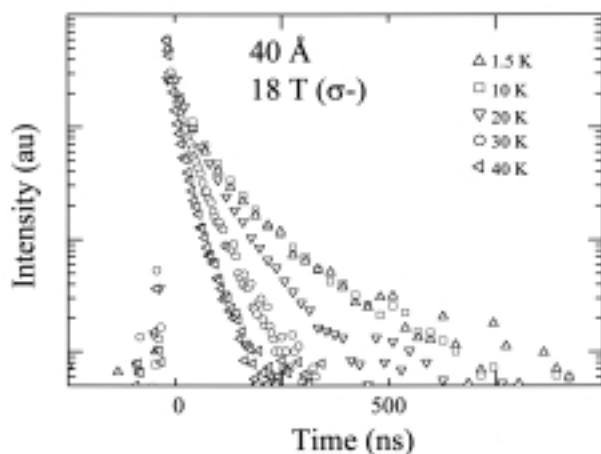


Figure 2. Decays of σ^- polarized photoluminescence for 40 Å diameter CdSe QDs at a range of temperatures from 1.5 to 40 K and at a field of 18 T. The same qualitative behavior is observed at fields from 0 to 18 T and for both σ^+ and σ^- polarizations.

for temperatures $T = 1.5$ -40 K. While we cannot be quantitative due to the non-exponential nature of the decay, it appears that some process analogous to thermal activation governs the temperature dependence. As the temperature is increased the temperature dependence of the luminescence decay is very weak until a threshold, above which the recombination time rapidly drops.

Photoluminescence-Linewidth-Derived Exciton Mass for InGaAsN Alloys

Jones, E.D., Sandia National Laboratory

Bajaj, K.K., Emory Univ., Physics

Tozer, S.T., NHMFL

Wei, X., NHMFL

We report a measurement of the variation of the value of the linewidth of an excitonic transition in InGaAsN alloys (1 and 2% nitrogen) as a function of hydrostatic pressure using photoluminescence spectroscopy. We find that the value of the excitonic linewidth increases as a function of pressure until about 100 kbars after which it tends to saturate. This change in the excitonic linewidth is used to derive the pressure variation of the reduced mass of the exciton using a theoretical formalism which is based on the premise that the broadening of the excitonic transition is caused primarily by compositional fluctuations in a completely disordered alloy. The variation of the excitonic reduced mass thus derived is compared with that recently determined using a first-principles band structure calculation based on local density approximation.

We briefly outline the basic ideas underlying the theory of excitonic linewidth in alloys. Excitonic transitions in semiconductor alloys as observed in optical measurements such as PL, PL excitation, and modulated reflectance are considerably broader than those observed in their binary components. The broadening mechanism has been attributed to compositional disorder which is inevitably present in these kinds of systems. The physical origin of the excitonic line broadening due to compositional disorder lies in the fact that the average alloy

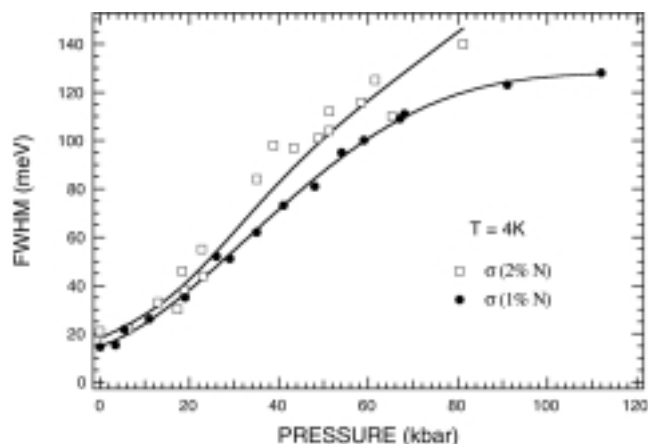


Figure 3. The pressure dependence of the FWHM photoluminescence linewidth for the 1% nitrogen (filled circles) and the 2% nitrogen (open squares) InGaAsN structures.

composition inside the volume occupied by the exciton is different from that inside the volume of another exciton in a different spatial region of the alloy. Within the framework of the virtual crystal approximation, the conduction and valence-band edges sampled by the exciton are determined by the local alloy composition. Therefore, excitons in different spatial regions have different optical transition energies, thus leading to inhomogeneous broadening of the transition energy. Here we implicitly assume that the exciton localization is entirely a result of the bandgap energy variations due to the random alloy fluctuations. Because of the large values of the variation of bandgap energy with composition for InGaAsN, motional averaging and other linewidth effects due to the thermal motion of the free exciton are neglected. Furthermore, because the bandgap offset between GaAsN and GaAs for the 1 and 2% nitrogen alloys is small the contributions to the alloy fluctuation theory of line broadening by fluctuating valence-band hole energies is also ignored.

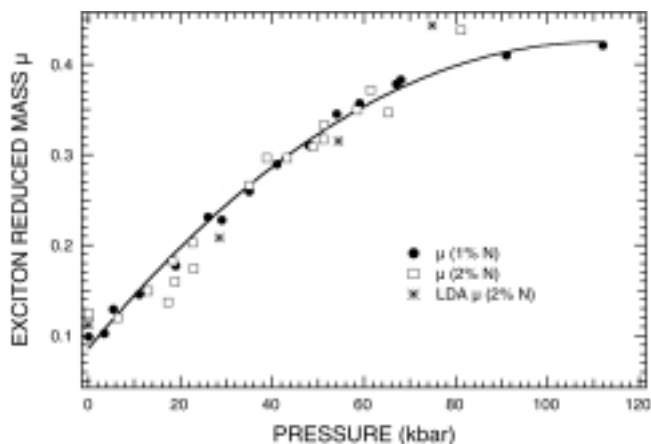


Figure 2. Exciton reduced effective masses versus pressure for 1% nitrogen (filled circles) and 2% nitrogen (open squares) samples using the FWHM data shown in Figure 1. The smooth curve drawn through the mass data is meant to be an aid to the eye. The stars are the pressure dependent LDA calculated reduced mass.

The reduced mass of the exciton as a function of pressure is derived from the observed variation of the excitonic linewidth using a theoretical formalism which is based on the broadening of the excitonic transition caused by the potential fluctuations in the alloy. Figure 1 shows the pressure dependence of the FWHM for the 1% (closed circles) and 2% (open squares) at $T = 4$ K. Figure 2 shows the exciton reduced effective masses μ versus pressure for 1% nitrogen (solid circles) calculated from the 4-K FWHM data shown in Figure 1. The open squares are for 2% nitrogen. The smooth curve drawn through the 1% nitrogen mass data (open circles) is meant to be an aid to the eye. The open triangles are the pressure dependent local density approximation calculated reduced mass.

Electron Cyclotron Resonance of 2DEG in Diluted Magnetic Semiconductor Heterostructures

Karczewski, G., Polish Academy of Sciences, Warsaw
 Wojtowicz, T., Polish Academy of Sciences, Warsaw
 Wang, Y.J., NHMFL

In recent years one observes an increasing interest in modulation doped II-VI structures containing quantum wells made of diluted magnetic semiconductors (DMSs). The interest arises from the fact that these structures offer a unique opportunity for studying an effect of localized magnetic spins on highly mobile two-dimensional electron gas (2DEG), yielding particularly valuable insights into spin processes in low dimensional geometry. In addition, II-VI materials are known for very strong electron-electron Coulomb interactions.

The cyclotron resonance (CR) of (2DEG) in modulation doped Cd(Mn)Te/CdMgTe quantum wells was investigated in magnetic fields up to 18 T. The quantum structures were grown by molecular beam epitaxy (MBE) with a precise in-plane profiling of either QW width or n-type doping level. The resulting 2D-electron mobility reaches the level of 10^5 cm²/Vs and the typical 2DEG concentration is on the order of 10^{11} cm⁻², which is the world record for II-VI wide-gap semiconductors. It is worth noting that for the first time the quality of II-VI structures becomes comparable to the quality of good III-V QWs. The structures contain magnetic ions directly incorporated into the QWs allowing for the intriguing possibility of studying the physics of a mobile gas of electrons whose spins are strongly exchange-coupled to the localized magnetic moments of Mn ions.

With decreasing QW width we observed a significant increase of the in-plane effective mass, from $0.100 m_e$ for 20 nm wide CdTe QW to $0.107 m_e$ for 7.5 nm well. A simple theoretical model has been proposed to describe this dependence. For QWs containing Mn in the well region, besides the CR line an additional resonance is observed. Since the resonance energy only slightly depends on magnetic field (at $8 \text{ T} < H < 15 \text{ T}$) we assigned this line to the forbidden spin-flip transition. The giant spin splitting of 8 meV is due to the exchange interaction of mobile 2D electrons with localized magnetic moments of Mn ions. The narrow CdMnTe QWs exhibit a disorder-induced localization effect that appears to be strongly dependent on 2DEG concentration.

Non-Equilibrium Phenomena in Doped IV-VI Semiconductors and Related Theoretical Studies

Khokhlov, D., Moscow State Univ., Physics

Narrow-gap IV-VI semiconductors are one of the basic materials of the infrared optoelectronics. They are mainly used for the production of lasers and LEDs operating in the middle- and far infrared, and for construction of photodetecting arrays with a high number of elements as well. Special attention is attracted to the semi-magnetic semiconductors based on IV-VI groups. Doping with magnetic impurities provides modification of the semiconductor energy spectrum in magnetic fields. This circumstance allows one to tune the spectral response of the respective optoelectronic devices by means of magnetic field application.

Another important direction of research is investigation of impurity states arising in IV-VI upon doping. In some cases this doping results in appearance of completely new features of the material. For instance, the Fermi level pinning and the persistent photoconductivity effect at low temperatures have been observed previously in the lead telluride-based alloys doped with In and Ga. The impurity centers responsible for the above-mentioned effects, as well as for many others, are quite similar to the DX-centers in III-V's and II-VI's. The "DX-like" behavior of impurity centers has been observed in the lead telluride-based alloys doped with the rare-earth element, Yb, and transition metal, Cr. Both of them are magnetic impurities, and this circumstance introduces a great deal of specifics in the physics involved and, consequently, in the effects observed. For instance, preliminary experiments have shown that the position of the pinned Fermi level E_F in PbTe(Yb) may be tuned by variation of magnetic field. This result opens new possibilities both for the fundamental and applied aspects of the problem, such as observation of a magnetic field-induced acceptor-donor transition, construction of a magnetic field-tunable photovoltaic infrared photodetector, and many others.

The f-d interaction of magnetic ions in the lead telluride-based alloys doped with both transition and rare-earth elements may influence the Fermi level pinning and the persistent photoconductivity effects, especially in the presence of high magnetic field. In our experiments, we have performed transport and magnetic measurements of this kind of semiconductors: PbTe(Yb,Mn).

A giant negative magnetoresistance effect has been observed. The sample resistance at liquid helium temperature drops by at least 3 orders of magnitude when the magnetic field increases up to 5-6 T, with subsequent rise by about one order of magnitude as the field further increases to 17.5 T. The effect is observed up to $T = 35$ K. The negative magnetoresistance effect results from the field-induced shift of the Fermi level position from the tail of the impurity band to its central part providing transition from

activation-like to metallic-like behavior of resistivity. Further increase of magnetic field above a certain value, H_0 , results in an onset of the variable-range hopping regime. The hopping characteristic temperature T_0 depends on the magnetic field applied as $T_0 \sim (H - H_0)^{5/2}$.

It is important to note that this effect has never been observed in PbTe doped separately with Mn and Yb. It means that interaction of magnetic impurities plays a crucial role in appearance of this effect. One more indication of the importance of this interaction comes from magnetic measurements of PbTe(Yb,Mn).

We have measured magnetization as a function of magnetic field up to 5.5 T at $T = 5$ K and as a function of temperature at $H = 0.1$ T. While the $M(H)$ data taken at 5 K demonstrate paramagnetic behavior with some trend to saturation in the fields $H \sim 5$ T, the $M(T)$ curve looks non-trivial. The Curie-Weiss behavior is not observed indicating that the magnetic moments responsible for the paramagnetism are not localized. It has been shown previously that the samples investigated are extremely sensitive to the action of infrared illumination. We have demonstrated that the sample resistivity is very sensitive to the action of magnetic field, too. Therefore these materials can be used as infrared and magnetic field sensors simultaneously. To our knowledge, this combination is unique. A paper on the research described has been submitted to the Physical Review Letters.

In-Plane Magnetoluminescence of Modulation-Doped GaAs/Al_{0.3}Ga_{0.7}As Coupled Double Quantum Wells **IHRP**

Kim, Y., NHMFL/LANL

Perry, C.H., Northeastern Univ., Physics

Simmons, J.A., Sandia National Laboratory

In-plane magnetic field photoluminescence spectra from a series of GaAs/AlGaAs coupled double quantum wells (CDQW's) show distinctive doublet structures related to the symmetric and antisymmetric states. In the presence of in-plane magnetic fields, single particle dynamics dominate the interactions between the two-dimensional electron gases and there is a linear shift in the canonical momentum $\hbar k$ in one quantum well with respect to another. The primary effect is to produce a partial energy gap and a strong modulation of the in-plane conductance due to an anti-crossing of the k -dispersion curves as demonstrated by Simmons *et. al.*¹ In a recent theoretical investigation, Huang and Lyo² describe many different phenomena related to the in-plane magnetic field dependence of the photoluminescence (PL) spectra of CDQW's.

The magnetic field behavior of the upper transition (U) from the antisymmetric state strongly depends on sample mobility. In lower mobility samples (Figure 1 (b)), the upper transition energy shows an N -type kink with fields (namely a maximum followed by a minimum), whereas higher mobility samples

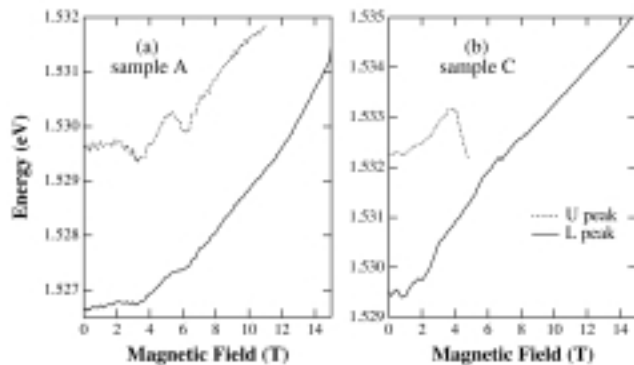


Figure 1. Transition energy vs. magnetic field plot. (a) For sample A which has higher mobility, the upper peak (U) runs in parallel to the lower peak (L) and disappears around 11 T. (b) For sample C (low mobility), the U peak shows N-type kink transition, namely a maximum followed by a minimum in the energies around 4 T.

have a linear dependence (Figure 1.(a)). The former is due to a homogeneous broadening of electron and hole states while degenerated k -dispersion curves separate along the y -direction and the results are in good agreement with theoretical calculations.²

¹ Simmons, J.A., *et al.*, Phys. Rev. Lett., **73**, 2256 (1994).

² Huang, D. and Lyo, S.K., Phys. Rev. B, **59**, 7600 (1999).

Positively Charged Magnetoexciton Transitions in a p -doped GaAs/AlGaAs Single Heterojunction IHRP

Kim, Y., NHMFL/LANL

Jiang, H.W., Univ. of California at Los Angeles, Physics and Astronomy

Lee, X., UCLA, Physics and Astronomy

It is known that two-dimensional electron gas undergoes Mott-Wannier (exciton) transitions in the presence of magnetic field beyond the quantum limit due to a charge localization.¹ We report a photoluminescence (PL) detected positively charged exciton (X^+) transition from a p -doped GaAs single heterojunction in magnetic fields to 60 T. Polarization dependent PL spectra at several selected fields are displayed in Figure 1 (a). As the field increased above the quantum limit (10.8 T), the free carrier transition smoothly changes into a neutral exciton (X^0) and positively charged exciton (X^+) transitions. In the inset of Figure 1 (a), X^+ transition is realized as a side peak of X^0 main transition. Above 25 T, these two peaks are well resolved. Figure 1 (b) displays transition energy versus magnetic field plot. The inset shows a relative binding energy of the observed X^+ to the neutral exciton transition. In comparison to its initial value ~ 12 T, the binding energy of the X^+ transition is doubled at 58 T. The variation of the X^+ binding energy in magnetic fields has B dependency. This is due to the fact that as the magnetic field increases the charged exciton orbit shrinks which increases Coulomb interaction within the excitonic complex. Theoretical studies expect² that the

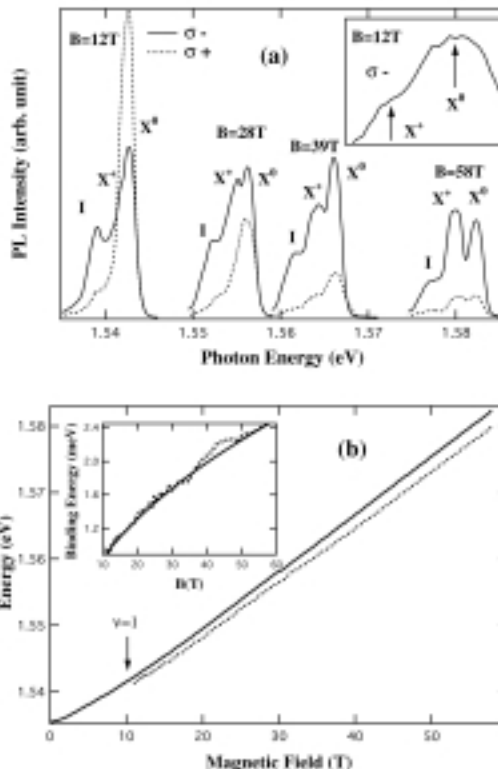


Figure 1. (a) Selected PL spectra for several magnetic fields. It is shown that the X^+ transition appears as side shoulder around 12 T (inset). (b) Transition energy versus magnetic field plot for σ^- transition. In the inset, relative binding energy (dotted line) of the X^+ is displayed which follows well with B fitting (solid line). The fitting function for the X^+ binding energy is $\Delta E = 0.085e^2/\ell_B$ (where $\ell_B = (ch/eB)$ is magnetic length).

increasing Coulomb interaction gives rise to B dependency for charged exciton transitions.

¹ Finkelstein, G., *et al.*, Phys. Rev. Lett., **74**, 976 (1995).

² Whittaker, D.M., *et al.*, Phys. Rev. B, **56**, 15185 (1997).

Topological Phase Diagram of Two-Subband Electron Systems in the High Magnetic Field Regime

Lee, X.Y., Univ. of California at Los Angeles, Physics and Astronomy

Jiang, H.W., UCLA, Physics and Astronomy

Kim, Y.M., NHMFL/LANL

Schaff, W., Cornell Univ., Electrical Engineering

For the considerable amount of work carried out in the variety of quantum Hall devices, most of the semiconductor heterostructures used for the experimental studies contain only one populated electronic subband. Even though studies of systems with two populated electric subbands have a long history, the inherent additional inter-subbands scattering has precluded two-subband system from being a primary

to study various aspects of quantum Hall effect. Recently, it has become increasingly apparent that, in a two-subband system, interaction of Landau levels of the two different subbands can lead to a very unusual topological phase diagram.¹

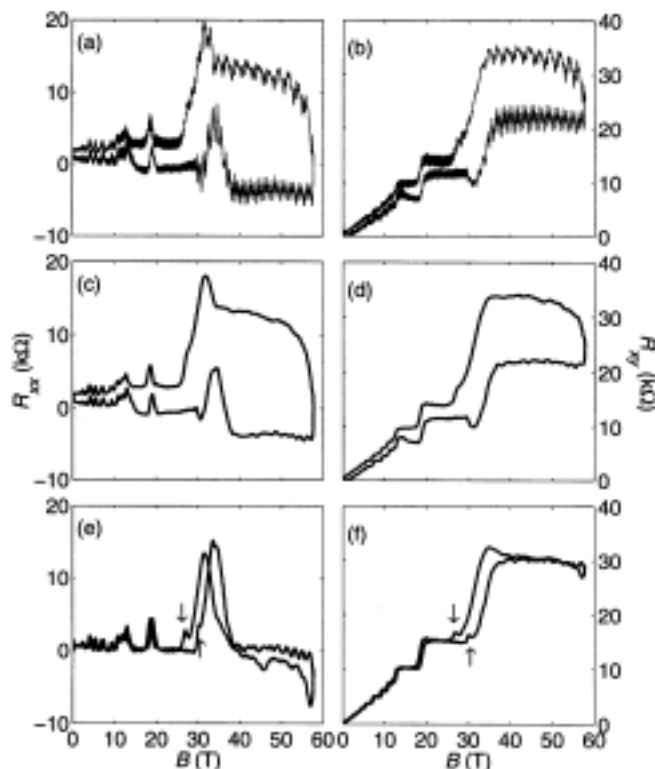


Figure 1. Magnetotransport data of a two-subband heterostructure at a gate voltage of -0.1 V obtained in the pulsed field. (a) and (b): raw data. (c) and (d): data after digital filtering. (e) and (f): data after subtraction of a pick-up signal background.

To explore further the consequences of Landau level interaction on the topology of the phase boundaries between different quantum Hall states, and to study the evolution of the delocalized states as levels moving towards and away from each other, we have extended our study in the high magnetic field regime where the spin degeneracy of all the Landau levels are well lifted. We have used a gated, high-density GaAs/AlGaAs single quantum well sample in which there are two populated subbands. A sequence magneto-transport studies was performed up to 60 T in the newly developed quasi-continuous magnet at LANL. We have obtained clean magneto-transport data (both R_{xx} and R_{xy} , see the figure) in the pulsed field in the presence of a gate voltage. The ability to vary the gate voltage of the device in the pulsed field setting allowed us to map out a high-field phase diagram in the density and magnetic field plane. We have observed interesting features in the vicinity of the level crossing of the $0\downarrow$ (spin-down state of the lowest Landau level of the first subband) and the $0\uparrow$ (spin-up state of the lowest Landau level of the second subband). We found, under certain values of gate-voltage, the very pronounced magneto-resistance peak between the $\nu=1$ and $\nu=2$ quantum Hall states splits into two peaks situated between 30 to 40 T. Preliminary analysis indicate that these anomalous features are likely related to the phase

transition from a spin unpolarized $\nu=2$ quantum Hall state to a spin-polarized $\nu=2$ quantum Hall state. The spin polarized may have a ferromagnetic broken symmetry.

¹ Lee, X.Y., *et al.*, Phys. Rev. Lett., **83**, 3701 (1999).

High Field EPR of the Strongly Coupled $\text{Cd}_{1-x}\text{Mn}_x\text{Se}$ and $\text{Cd}_{1-x}\text{Mn}_x\text{S}$ Magnetic Semiconductor Alloys

McCarty, A.D., NHMFL
Martins, G.B., NHMFL
Saylor, C., NHMFL
Furdyna, J.K., Univ. of Notre Dame, Physics
Brunel, L.-C., NHMFL

High field EPR proves to be a powerful tool for probing the magnetic interactions of magnetic semiconductors, and we have applied this technique to the investigation of two semiconductor alloy systems: $\text{Cd}_{1-x}\text{Mn}_x\text{Se}$ and $\text{Cd}_{1-x}\text{Mn}_x\text{S}$. The Mn^{2+} ions in these alloys are strongly coupled and the nature of the Mn^{2+} - Mn^{2+} interactions is revealed in the linewidth and resonance position of the EPR spectrum. These results demonstrate that there are two distinct regimes of inter-ion interactions. These regimes can be called “weak coupling regime” and “strong coupling regime”. The coupling is stronger in alloys with higher Mn^{2+} concentration ($x > 0.25$). For $\text{Cd}_{1-x}\text{Mn}_x\text{Se}$, alloys with Mn^{2+} concentrations $x = .08, .18, .26, .40, .46$ have been studied, and for $\text{Cd}_{1-x}\text{Mn}_x\text{S}$, the concentrations $x = .17, .20, .26, .38$ have been investigated. In the higher concentration alloys studied, there is a transition from the “weak coupling regime” at higher temperatures ($T > 40$ K) to the “strong coupling regime” at lower temperatures. These two regimes are distinguished by the linewidth dependence on the applied field. For the strongly coupled regime, the linewidth decreases with increasing applied

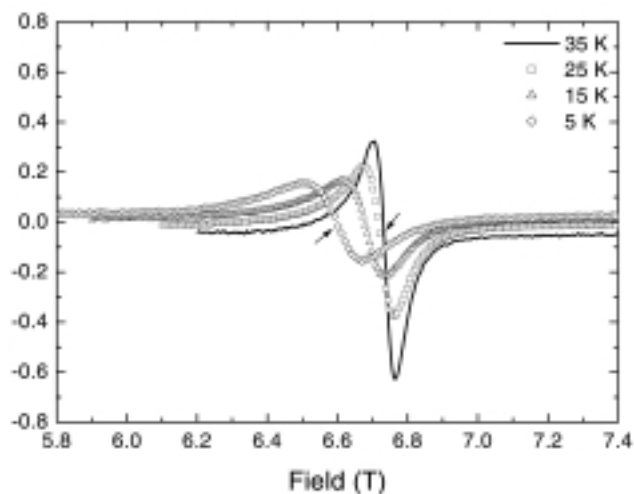


Figure 1. Spectra of $\text{Cd}_7\text{Mn}_3\text{S}$ at temperatures 35 K, 25 K, 15 K, 5 K and frequency of about 190 GHz demonstrating the shift in the resonance position to lower fields with decreasing temperature.

field. For the weakly coupled regime, the linewidth increases with increasing applied field.

For alloys with high Mn^{2+} concentrations, there is a shift in the resonance position to a lower field with decreasing temperature. Previous EPR work has provided an indication that the resonance position shifts to lower fields as the temperature is lowered.^{1,2,3,4} Because the lines in those earlier studies were extremely broad little could be said about what was happening. In the present work, high fields allow for the observation of the resonance position shift at lower temperatures than were previously possible.

- 1 Kremer, R.E. and Furdyna, J.K., Phys. Rev. B, **32**, 5591 (1985).
- 2 Kremer, R.E. and Furdyna, J.K., J. Magn. Magn. Mater. **40**, 185 (1983).
- 3 Sayad, H.A. and Baghat, S.M., Phys. Rev. B, **31**, 591 (1985).
- 4 Oseroff, S.B., Phys. Rev. B, **25**, 6584, (1982).

Energy Behavior with Magnetic Field of Negatively Charged Magneto-Excitons in a GaAs/AlGaAs Quantum Well

Munteanu, F.M., NHMFL/LANL and Northeastern Univ.,
Physics

Rickel, D.G., NHMFL/LANL

Kim, Y., NHMFL/LANL

Perry, C.H., Northeastern Univ., Physics

Simmons, J.A., Sandia National Laboratory

Reno, J., Sandia National Laboratory

The formation and behavior with magnetic field of the negatively charged magneto-excitons (X^-) in modulation doped GaAs/AlGaAs quantum heterostructures has received increased attention recently, both experimentally and theoretically. Their formation in the quasi two dimensional (2D) case is facilitated over 3D systems as a result of the confinement. The energy separation between the X^- and the neutral exciton (X^0) lines was found¹ to increase with magnetic field for both the singlet X_S^- and the triplet X_T^- state. Whittaker and Shields² showed that in order to obtain the correct binding energy of the X^- states, one must include in the calculations the presence of the higher energy subbands and higher Landau levels (LLs). As a result, they predicted for a 100Å QW that the X_S^- and the X_T^- states should cross at magnetic field of about 35 T.

The sample that we investigated using photoluminescence spectroscopy was a 200Å GaAs/Al_{0.55}Ga_{0.45}As modulation doped single QW, with a dark electron density of $1.2 \times 10^{11} \text{ cm}^{-2}$ and mobility higher than $3 \times 10^6 \text{ cm}^2/\text{Vs}$. With constant laser illumination (at 632.8 nm) during the measurements, the 2DEG density increased to $1.58 \times 10^{11} \text{ cm}^{-2}$. A quasi-continuous magnet at NHMFL-LANL provided a magnetic field from 0 to 60 T. The temperature studies were made at 1.5 K to 370 mK.

In Figure 1 the evolution of the X^0 , X_S^- and X_T^- lines for the 200Å QW is shown as a function of magnetic field. The most

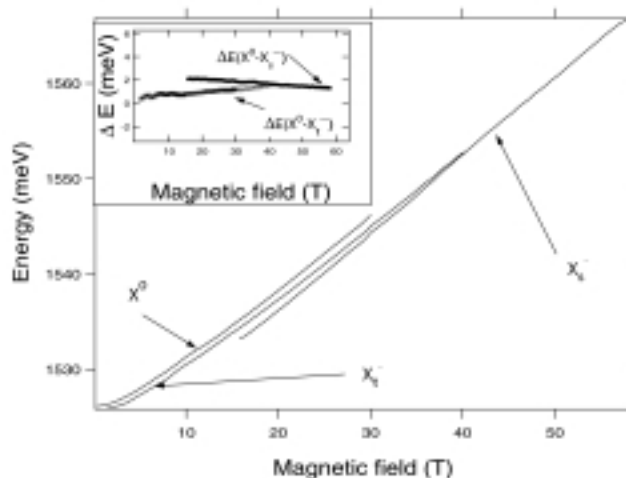


Figure 1. The evolution of the X^0 , X_S^- and X_T^- peaks with magnetic field for the 200Å QW. Around $B=40$ T, there is a crossing of the singlet and triplet transitions. Inset: the energy separations between X^0 and X_S^- , $E(X^0-X_S^-)$ and X^0 and X_T^- , $E(X^0-X_T^-)$, peaks are presented as a function of magnetic field.

important thing of note is that at a field of about 40 T, we observe a crossing of the X_S^- and X_T^- states. Beyond 40 T only one peak could be resolved.

This result is more clearly shown in the inset of Figure 2. It presents the energy separation between X^0 and X_S^- peaks, $E(X^0-X_S^-)$, and X^0 and X_T^- peaks, $E(X^0-X_T^-)$. It can be seen that in the X_T^- case, $E(X^0-X_T^-)$ increases with field from 0.4 meV at 2 T to 1.2 meV at 30 T, while the energy separation between the X_S^- and X^0 states $E(X^0-X_S^-)$ decreases slowly from 2.1 meV at $B=15.7$ T to 1.4 meV at $B=58$ T.

These results prove the important role played by the higher Landau levels in the binding energy of the X^- . This role is more significant in the case of the narrower QWs.

- 1 Shields, A.J., *et al.*, Phys. Rev. B, **52**, 7841 (1995).
- 2 Whittaker, D.M. and Shields, A.J., Phys. Rev. B, **56**, 15185 (1997).

Photoluminescence Detected Doublet Structure in the Integer and Fractional Quantum Hall Regime

Munteanu, F.M., NHMFL/LANL and Northeastern Univ.,
Physics

Rickel, D.G., NHMFL/LANL

Perry, C.H., Northeastern Univ., Physics

Kim, Y., NHMFL/LANL

Simmons, J.A., Sandia National Laboratory

Reno, J., Sandia National Laboratory

One of the most significant phenomenon that occurs in the FQHE regime is the emergence of low-lying charge density (CD) waves that display characteristic magneto-roton (MR)

minima at a wave vector close to the inverse magnetic length. At large wave vector, neutral CD waves excitations consist of pairs of fractionally charged quasiparticles that are associated with the energy gaps of the Integer Quantum Liquid.

In this report, we present the results of MPL measurements of a MBE grown high quality modulation-doped GaAs/Al_{0.3}Ga_{0.7}As single heterojunction (SHJ). The polarized spectra that we observed revealed the formation of a doublet structure at a filling factor close to $\nu=3/2$ and the persistence of this effect to the highest magnetic field utilized. The GaAs/Al_{0.3}Ga_{0.7}As SHJ used for the measurements had a dark electron density of $1.2 \times 10^{11} \text{cm}^{-2}$ and a mobility higher than $3 \times 10^6 \text{cm}^2/\text{Vs}$. With constant laser illumination during the measurements, the 2DEG density increased to $2.1 \times 10^{11} \text{cm}^{-2}$. Using a quasi-continuous magnet, field was varied from 0 to 60 T, while the temperature was changed from 1.5 K to 450 mK.

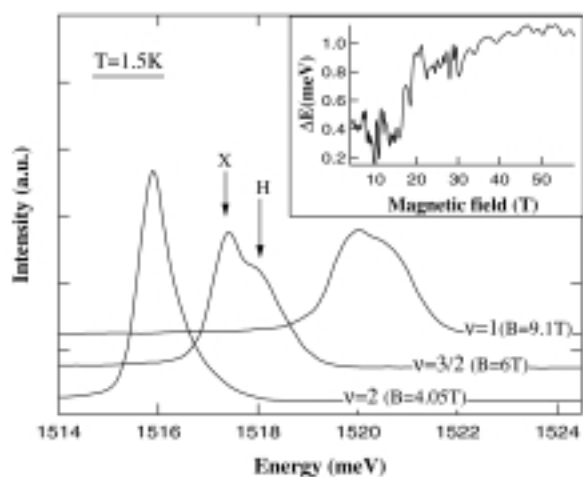


Figure 1. Unpolarized MPL spectra at 1.5 K for three different filling factors. The appearance of the doublet structure is resolved at $\nu=3/2$. The inset shows the energy difference (ΔE) between the “H” and “X” peaks as a function of magnetic field to 58 T.

In Figure 1, we show the unpolarized spectra obtained at a temperature of 1.5K at the filling factor $\nu=2, 3/2$ and 1. The E0-hh (neutral exciton) peak that appears at $\nu=5$ ($B=1.82$ T) shows a splitting for $2 > \nu > 1$ and this is clearly seen in the spectrum at $\nu=3/2$. The doublet structure is labeled X and H, where H refers to the higher energy split-off peak. The two peaks once formed are present for the whole range of magnetic fields examined. The difference in the energies (ΔE) between H and X as a function of magnetic field is shown in the inset in Figure 1. It can be seen that ΔE has a sudden increase in the region of $\nu=1/2$ (16 to 19 T) and then saturates for fields higher than 30 T. The value of the separation (0.4-1.2 meV) is close to the FQHE quasiparticle-quasihole separation gap energy (about 1 meV). It does not scale as the magnetic energy ($B^{1/2}$) but rather follows an almost linear behavior in the range $1 > \nu > 1/3$. The intensity oscillations of the X and H peaks at various integer and fractional filling factors were generally opposite in nature and were obviously interrelated. At low temperatures, the H peak becomes dominant. The interpretation of the higher energy H peak of the exciton

doublet structure remains inconclusive, despite the fact that its behavior with magnetic field presents some similarities with the predicted magneto-roton formation.

Photoluminescence Detected Enhancement of the Electron-Hole Exchange Interaction in a Quantum Well

Munteanu, F.M., NHMFL/LANL and Northeastern Univ., Physics

Rickel, D.G., NHMFL/LANL

Kim, Y., NHMFL/LANL

Perry, C.H., Northeastern Univ., Physics

Simmons, J.A., Sandia National Laboratory

Reno, J., Sandia National Laboratory

Enhancement of the electron-hole exchange interaction (EHExI) in a quantum well structure was carefully reviewed by Chen *et al.*¹ This increase is due to the 2D confinement compared with its value in bulk material. For this reason, the fine structure of the heavy-hole exciton (HHE) at $B=0$ T consists of two transitions. The higher energy one is dipole allowed and the lower energy one (with the energy equal to the energy of the HHE in the absence of the EHExI) dipole forbidden.

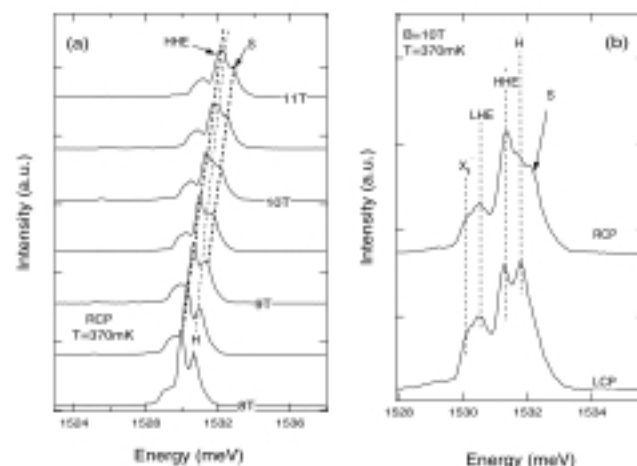


Figure 1. (a) The RCP spectra show the appearance of the S peak at $B \sim 9$ T; (b) The RCP and LCP spectra at $B=10$ T. The S peak is absent in the LCP spectrum.

Here we report a series of circularly polarized magneto-photoluminescence (MPL) measurements on a high-quality GaAs/AlGaAs QW with a well width of 200 Å. The experiments were performed in magnetic fields up to 60 T and at temperatures of 370 mK. The appearance of a high-energy peak in the RCP polarization, in addition to the observed HHE, is considered to be a result of localization enhanced EHExI.

Figure 1a shows some right circular (RCP) polarized spectra taken in the range 8 to 11 T at a temperature of about 370

mK. The most important observation is the appearance of a supplementary peak, labeled S. This peak is absent in the LCP spectra as illustrated in Figure 1b. We interpret this new peak S as evidence of the enhancement of the EHEXI. Around $B=25$ T, the intensity of the S peak became very small as a result of depopulation of the $-1/2$ electronic level. We find that when the HHE and S peaks are extrapolated to zero magnetic field, the energy difference between them is close to zero, as calculated.² Due to this small separation energy, we were unable to resolve the formation of the S peak below $B=9$ T. The electron effective g-factor was determined to be 3.7 times higher than its bulk value as a result of the EHEXI enhancement.

¹ Chen, Y., *et al.*, Phys. Rev. B, **37**, 6429 (1988).

² Andreani, L.C. and Bassani, F., Phys. Rev. B, **41**, 7536 (1990).

Enhanced Effective Mass at $\nu=1$ in $\text{Zn}_{1-x-y}\text{Cd}_x\text{Mn}_y\text{Se}$ Heterostructures

IHRP

Ng, H.K., FSU, Physics
 Leem, Y.A., FSU, Physics
 Storr, K., FSU, Physics

This report is on the cyclotron resonance (CR) measurements performed on two-dimensional electron gases (2DEGs) in modulation-doped magnetic semiconductor heterostructures, $\text{Zn}_{1-x-y}\text{Cd}_x\text{Mn}_y\text{Se}$, and also on the non-magnetic analogues, $\text{ZnSe}/\text{Zn}_{1-x}\text{Cd}_x\text{Se}$ and ZnTe/CdSe . The latter compounds provide a valuable comparison to the magnetic compounds. The samples have carrier densities ranging from 1 to 4×10^{11} cm^{-2} and mobilities as high as 42,000 $\text{cm}^2/\text{V}\cdot\text{s}$ for the non-magnetic samples.

The experiments were performed using (optical) Fourier Transform spectroscopy and with fields from 4 T to 31 T. In

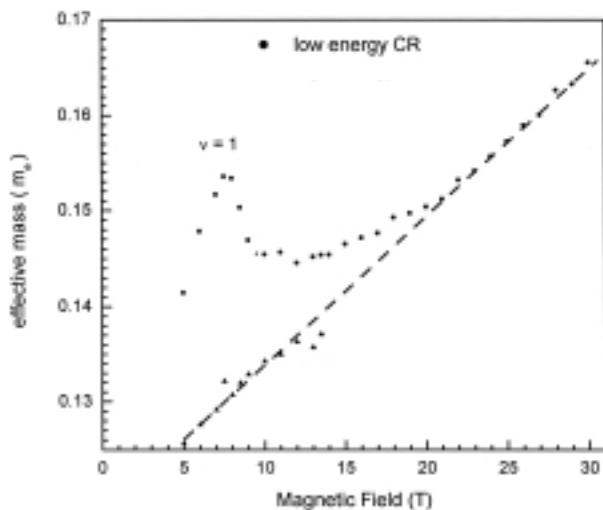


Figure 1. Effective mass obtained from the cyclotron resonance.

Figure 2 the effective mass obtained from the absorption line is plotted as a function of magnetic fields. The figure shows many interesting features. At filling factor of $\nu = 1$, there is a strong mass enhancement. The enhancement is about 10% and is more than an order of magnitude stronger than that observed in GaAs. In GaAs, the mass enhancement shows an oscillatory effect peaking at each integer filling factor and is only about 0.5%. There the effect is attributed to perturbation in the dynamic electron-electron interaction at the filling factor. Clearly, perturbation in electron-electron interaction is too weak to explain the large mass increase at $\nu = 1$ in our case.

The second interesting feature is the increase in mass as the magnetic field is increased. The increase can be understood as the resonant polaron coupling since for ZnSe the longitudinal-optical (LO) phonon is at 254 cm^{-1} . The high field data can be fitted for a 2D electron gas model with the Frolich electron-phonon coupling constant, $\alpha = 0.215$.

Acknowledgments: Work at FSU is supported in part by the State of Florida through the Center for Materials Research and Technology, and the NHMFL In-House Research Program, and the NHMFL's NSF contract (DMR-9527035).

Strongly Anisotropic Electronic Transport at $\nu = 9/2$ and $5/2$ under a Tilted Magnetic Field

Pan, W., Princeton Univ., Electrical Engineering/NHMFL
 Du, R.R., Univ. of Utah, Physics/NHMFL
 Stormer, H.L., Columbia Univ., Physics and Applied Physics/Bell Labs, Lucent Technologies
 Tsui, D.C., Princeton Univ., Electrical Engineering
 Pfeiffer, L.N., Bell Labs, Lucent Technologies
 Baldwin, K.W., Bell Labs, Lucent Technologies
 West, K.W., Bell Labs, Lucent Technologies

In higher Landau levels ($\nu > 4$) at half-filling of either spin level ($\nu = 9/2, 11/2, 13/2, 15/2$, etc.) the Hall resistance, R_H , is erratic and diagonal resistance, R , exhibits a strongly anisotropic behavior, showing a strong peak in one current direction (R_{xx}) and a deep minimum when the current direction is rotated by $\sim 90^\circ$ within the plane (R_{yy}). The origin of these states remains unclear. They are believed to arise from the formation of a striped electronic phase or an electronic phase akin to a liquid crystal phase. We have performed tilted magnetic field experiments in a single-subband heterojunction on the states at these fillings and observed very different behavior for different states.¹ For the states at $\nu = 9/2$ and $11/2$, the initial direction of the in-plane anisotropy is overwritten by the in-plane field, B_{ip} . Depending on the tilt direction, and therefore the direction of the in-plane field, the easy direction and the hard direction either remain in place or trade places with increasing B_{ip} [Figure 1(a) and 1(c)]. Surprisingly, the $\nu = 5/2$ and $7/2$ states, which do not show any initial in-plane anisotropy become strongly anisotropic under tilt [Figure 1(b) and 1(d)], similar to the states

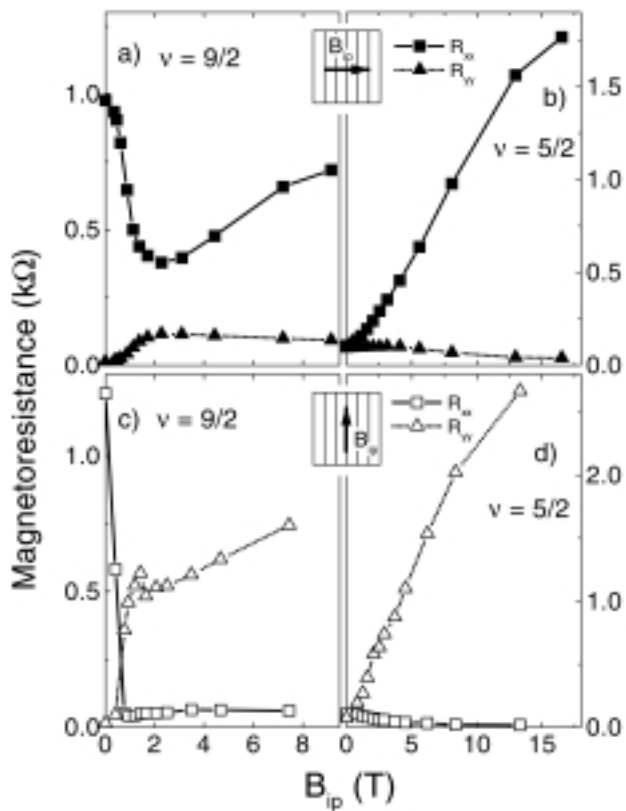


Figure 1. R_{xx} and R_{yy} as a function of in-plane magnetic field, B_{ip} , at $\nu = 9/2$ and $5/2$ for two tilt directions.

at $\nu = 9/2$ and $\nu = 11/2$. In all cases, under high tilt angles, it is exclusively the relative direction of current and in-plane magnetic field that determines whether R shows a minimum or a maximum.

¹ Pan, W., *et al.*, Phys. Rev. Lett., **83**, 3530 (1999).

Field and Wavelength Dependence of Optically Pumped NMR in Bulk InP

Patel, A., UF, Chemistry
 Pasquet, O., UF-France REU
 Bharatam, J., UF, Chemistry
 Hughes, E.L., UF, Chemistry
 Bowers, C.R., UF, Chemistry/NHMFL

We have measured the magnetic field dependence and wavelength dependence of optically pumped NMR in InP single crystal. The field dependence was mapped using a field cycling procedure implemented on a resistive type Bitter magnet where the possibility to achieve fast field sweeps (c.a. 0.5 T/s) was exploited. The rapid ramp rate permits the transition between different magnet fields to be completed in a time short compared with the nuclear spin-lattice relaxation time in the absence of optical pumping light. The 0 to 25 T field dependence of optical pumping with unpolarized light in InP and GaAs is shown in the Figure 1. The NMR enhancement increases sharply from zero

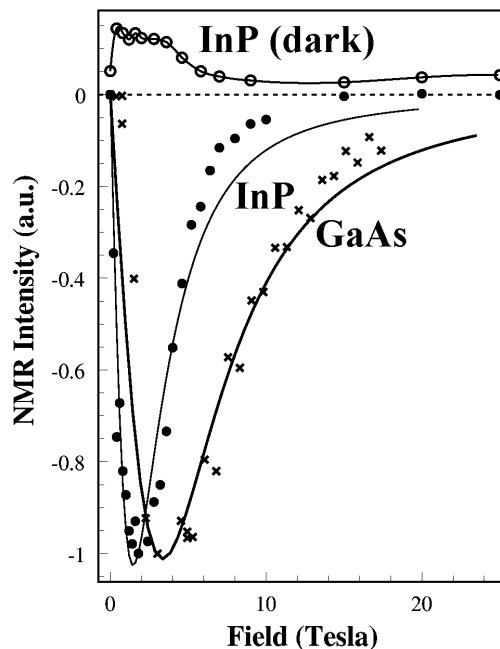


Figure 1. Magnetic field dependence of the optically enhanced NMR signal in undoped GaAs (crosses) and InP.

at 0 T to a maximum NMR enhancement at 1.7 T in the case of InP, while in GaAs the maximum enhancement was obtained at 3.0 T. Beyond these maxima the enhancement gradually decreases with increasing field in both materials. Negligible enhancement is obtained at >15 T.

The field dependence of optical pumping was modeled by hyperfine cross-relaxation with spin-diffusion. Assuming literature values for the g -factors, least squares fitting of the relaxation/diffusion model to the experimental field and polarization dependences yielded the correlation time τ_c for electron-nuclear hyperfine fluctuations. The experimental observation that the maximum optical pumping enhancement occurs at lower magnetic field in InP compared to GaAs was explained using the theory for hyperfine cross-relaxation. The theory predicts that the optimal NMR signal enhancement should be obtained at a field $B_{max} = |g_e \gamma_e \tau_c|^{-1}$, where g_e is the electron g -factor and γ_e is the gyromagnetic ratio of the electron.

The phase information of the optical pumping enhanced NMR signal was also interpreted. When irradiated with unpolarized pumping light, the enhanced ^{115}In NMR signal was observed to be emissively phased with respect to the thermal equilibrium absorption NMR signal. This was shown to be consistent with a dipolar hyperfine cross-relaxation mechanism in InP, while in GaAs, the emissive phase is consistent with a scalar mechanism since the g -factor has the opposite sign.

The optical pumping field dependence study in bulk GaAs and InP provided the first explanation for the occurrence of nuclear spin polarization enhancement using unpolarized rather than circularly polarized light. The experiments confirmed the mechanism and dynamics of cross-relaxation and provide guidance on how to optimize the conditions to potentially

observe hyperfine fields due to electrons trapped at shallow donor sites where dynamic nuclear polarization occurs.

Magnetization Measurements on the III-VI Diluted Magnetic Semiconductor $\text{Ga}_{1-x}\text{Mn}_x\text{S}$ at High Fields

Pekarek, T.M., Univ. of North Florida, Natural Sciences
Hughes, S.B., Stanton Coll. Prep., Physics
Graf, A.T., Univ. of North Florida, Natural Sciences
Duffy, M., Univ. of North Florida, Natural Sciences
Maymi, C., Univ. of North Florida, Natural Sciences
Crooker, B.C., Fordham Univ., Physics
Miotkowski, I., Purdue Univ., Physics
Ramdas, A.K., Purdue Univ., Physics

Research on the new layered III-VI Diluted Magnetic Semiconductors (DMS), which have a two-dimensional structure similar to mica, complements the enormous progress in the II-VI DMS and the more recent efforts in the Mn doped III-V DMS systems. The III-VI semiconductors GaSe, InSe, and GaTe have received considerable interest in the last few years because they have remarkable nonlinear optical properties and are promising materials for photoelectronic applications. GaS is comparatively uninvestigated and, to our knowledge, no work has been reported on Mn in GaS.

Little is known about the magnetic properties of this new class of layered III-VI DMS except for a pair of publications^{1,2} that presents magnetization data in fields below 6 T on $\text{Ga}_{1-x}\text{Mn}_x\text{Se}$ and $\text{Ga}_{1-x}\text{Mn}_x\text{S}$, respectively. The prominent broad peak from 119 to 195 K in $\text{Ga}_{1-x}\text{Mn}_x\text{Se}$, ascribed to direct Mn-Mn pairs, is absent in $\text{Ga}_{1-x}\text{Mn}_x\text{S}$. In this temperature range, $\text{Ga}_{1-x}\text{Mn}_x\text{S}$ is Curie-Weiss like with $\text{Jeff}/k\text{B} = -50$ K. $\text{Ga}_{1-x}\text{Mn}_x\text{S}$ shows a cusp at 10.9 K for an $x = 0.066$ sample similar to the spin-glass transition observed in the II-VI DMS.

Magnetization measurements on $\text{Ga}_{1-x}\text{Mn}_x\text{S}$ were made at the NHMFL in fields up to 30 T using the cantilever method. These measurements show that the magnetization saturates significantly more slowly than a standard paramagnet and suggest that the ground multiplet for the singlet Mn ions has an energy/kB gap around 20 K between a non-magnetic ground state and magnetic excited states. Theoretical work is underway to investigate the underlying energy levels that give rise to the observed magnetic behavior in this new layered III-VI DMS system.

¹ Pekarek, T.M., *et al.*, J. Appl. Phys., **83**, 7243 (1998).

² Pekarek, T.M., *et al.*, J. Appl. Phys., in press (2000).

Magnetic Field Effects on Indirect Excitons in GaAs Coupled Quantum Wells

Snoke, D., Univ. of Pittsburgh, Physics and Astronomy
Negoita, V., Univ. of Pittsburgh, Physics and Astronomy
Eberl, K., Max Planck Institut fuer Festkoerperforschung, Stuttgart, Germany
Chang, Y.C., Univ. of Illinois at Urbana-Champaign, Physics

Coupled quantum wells are a fascinating nonlinear system because when electric field is applied normally to the quantum well planes, electrons and holes created by photoexcitation are trapped in two different, adjacent parallel planes with weak coupling between them. This leads to several interesting effects. First, the luminescence decay time is considerably lengthened, up to 100 ns¹ in these samples, because the electron-hole wavefunction overlap becomes small. Second, the photon energy of the lowest allowed transition is strongly dependent on the applied electric field, an effect known as the quantum-confined Stark effect.^{1,2} Third, because the interaction of carriers in a single well is strong while the interaction between the wells is weak, there are strong renormalization effects on the carrier energies.³

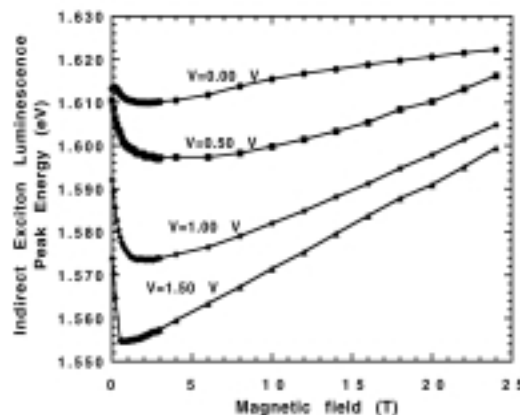


Figure 1. Photoluminescence energy for a GaAs/ $\text{Al}_3\text{Ga}_7\text{As}$ coupled quantum well structure with well thickness of 60 angstroms and barrier thickness of 42 angstroms.

We have studied the effect of the magnetic field on the indirect excitons in coupled quantum wells in GaAs at magnetic fields up to 25 T. An unexpectedly large red shift of the indirect exciton line occurs at relatively low magnetic field.⁴ This shift depends strongly on the electric field applied parallel to the growth direction. Our tentative explanation of this effect at this time is that the weak magnetic field causes electron-hole localization into magnetoexcitons, which strongly alters the Coulomb interaction of the carriers.

¹ Negoita, V., *et al.*, Phys. Rev. B, **60**, 2661, (1999).

² E.g., Andrews, S.R., *et al.*, Phys. Rev. B, **37**, 8198 (1988).

³ Negoita, V., *et al.*, "Huge Density-Dependent Blue Shift of Indirect Excitons in Biased Coupled Quantum Wells," Phys. Rev. B, **61**, 2779 (2000).

⁴ Negoita, V., *et al.*, "Strong Red Shift of Indirect Exciton Luminescence in Low Magnetic Field," Solid State Comm., **113**, 437 (2000).

A New ESR Test for Skyrmions in the Regime of the Quantum Hall Effect

Vitkalov, S.A., UF, Chemistry
 Bowers, C.R., UF, Chemistry
 Simmons, J.A., Sandia National Laboratories
 Reno, J.L., Sandia National Laboratories

A new ESR method was devised to probe for skyrmion excitations of the 2DES which is analogous to the tilted field method devised by Fang and Stiles and more recently employed to by Eistenstein et al. to investigate g-factor enhancement due to skyrmions at $\nu=1$. The advantage of the ESR method is that the experiment is conducted at constant temperature and magnetic field, and involves no change of the orientation of the sample in the field. Since the method is based on transport, selectivity for the extended states of the 2D electron system is achieved because only the extended states contribute to the signal.

In the new ESR method the number of spin flips s comprising a skyrmion excitation is based on the effect of local nuclear hyperfine fields on the 2D longitudinal conductivity, σ_{xx} . As in previous thermal activation determinations of the energy gap in the lowest Landau level, the analysis is based on the assumption that the gap at thermal equilibrium can be separated into two terms, $E_{eq} = \Delta_0 + s |g| \mu_B (B_0 + B_n)$, where Δ_0 is the exchange energy due to the e-e interaction and $s |g| \mu_B B_0$ is the Zeeman energy due to the applied field B_0 . Note that an additional local nuclear field term has been included, $B_n = A [I_z]$, where A is the collective hyperfine coupling constant and $[I_z]$ is the nuclear spin polarization. Ordinarily this term can be neglected, but in the new method it is significantly enhanced using the Overhauser (or DNP) effect. The enhanced local nuclear field $B_n^{DNP} = A [I_z]^{DNP}$ persists on the time scale of the nuclear spin relaxation time and can be monitored by ESR field sweeps, as illustrated in the figure. The change in the local nuclear field is given by $\Delta B_n = A ([I_z]^{DNP} - [I_z]^{EQ})$. Since the magnitude of the enhanced nuclear field is an appreciable fraction of the external magnetic field, there is a significant change in the activation energy. It is easily shown that the relative change in conductivity is proportional to the change in the nuclear hyperfine field: $\Delta \sigma_{xx} / \sigma_{xx} = -s |g| \mu_B \Delta B_n / 2kT$. The DC conductivity change $\Delta \sigma_{xx} / \sigma_{xx}$ is measured between the conductivity minima before and after DNP enhancement, while electrically detected electron spin resonance (ESR) is employed to determine the change of the nuclear field, ΔB_n . The number of spin flips in the thermally activated excitation is determined by plotting $\Delta \sigma_{xx} / \sigma_{xx}$ versus $-|g| \mu_B \Delta B_n / 2kT$.

The new transport/ESR hybrid has been demonstrated in the study of skyrmion excitations at $\nu=1$ in two different low electron density GaAs/AlGaAs multiple quantum well sample under conditions which should be well within the skyrmion regime. In both samples, the Zeeman contribution to the energy splitting in the lowest Landau level was found to correspond to single spin flips ($s=1$) rather than skyrmions ($s>1$). Future

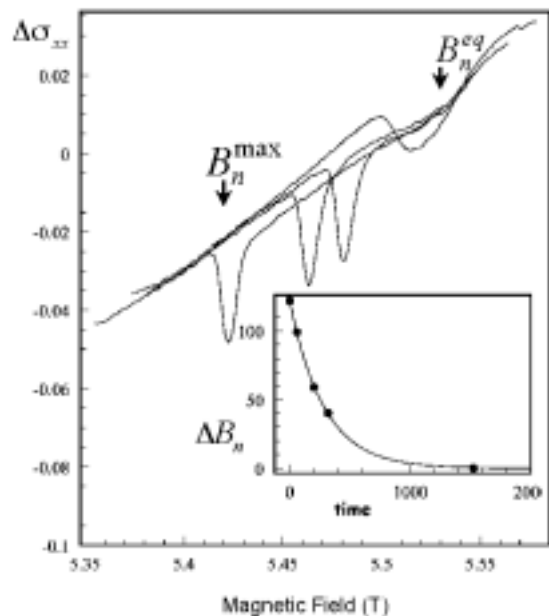


Figure 1. Conductivity detection of ESR spectra as a function of time after DNP. The ESR peak exhibits an Overhauser shift due to the enhanced nuclear spin polarization. Inset: Decay of Overhauser shift due to nuclear spin relaxation.

work will entail comparative studies against other experimental methods, such as Knight shift NMR measurements, and activated transport in a tilted field.

Resonant Magnetopolaron Effect in Modulation-Doped GaAs/AlGaAs Quantum Wells at High Magnetic Fields

Wang, Y.J., NHMFL
 McCombe, B.D., State Univ. of New York at Buffalo,
 Physics
 Jones, E.D., Sandia National Laboratories
 Peeters, F.M., Univ. of Antwerpen, Physics

Electron cyclotron resonance (ECR) has been measured to study the interaction between electrons and phonons, which has a strong effect on the electronic properties of semiconductors. The experiments are carried out in magnetic fields up to 32 T in two sets of heavily modulation- δ -doped GaAs/Al_{0.3}Ga_{0.7}As quantum-well samples.

Little effect on ECR was observed in either of the two samples in the first set in the region of resonance with the GaAs longitudinal optical (LO) phonons. Above the LO phonon energy, E_{LO} , at $B > 27$ T, however, ECR exhibits a strong avoided-level-crossing splitting for both samples at energies close to $E_{LO} + (E_2 - E_1)$, where E_2 , and E_1 are the energies of the bottoms of the second and the first subbands, respectively. The energy separation between the two branches is large, reaching a minimum of about 40 cm^{-1} around 30.5 T for both samples. This splitting is due to a three-level resonance between the

second Landau level (LL) of the first electron subband and the lowest LL of the second subband plus a LO phonon. The large splitting in the presence of high electron densities is due to the absence of occupation (Pauli-principle) effects in the final states and weak screening for this three level process. Detailed calculations specifically for our two sample structures have been carried out to compare with the experimental results. The electron-phonon interaction and the influence of LL occupancy and screening on it are included in the calculation. Very good agreement between the calculated results and the experimental results is shown in Figure 1.

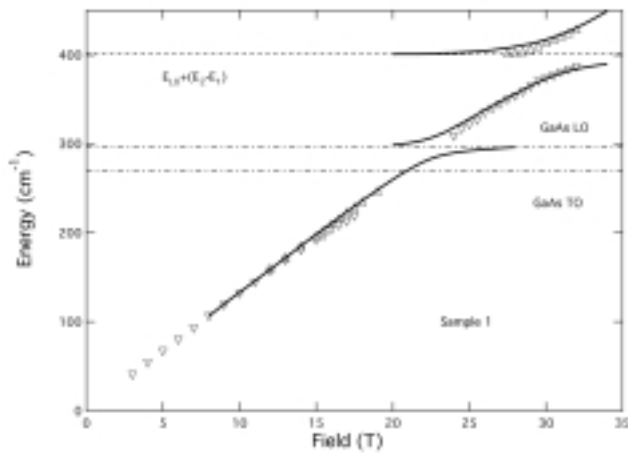


Figure 1. The comparison between the calculated results and the experimental data of CR transition energy vs. field for sample 1. The subband energy ($E_2 - E_1$) is calculated self-consistently.

Each of the three samples in the second set shows different CR behavior. Below the GaAs reststrahlen region, only one CR peak is resolved for all samples. Above the GaAs LO-phonon region ($B > \sim 23$ T), the three samples behave very differently. A sample of intermediate density ($7.5 \times 10^{11} \text{ cm}^{-2}$), sample B, shows two lines above 23 T; while the other two show one resonance at the different positions of the two frequencies for sample B. These two CR lines are due to the spin splitting. The reason that we observed two branches in sample B and one branch in the high and low density is a consequence of the blocking of the polaron interaction.

Zeeman Spectroscopy of GaAs/AlGaAs Quantum Wire Arrays

Woo, J.C., Seoul National Univ., Physics

Kim, D.H., SNU, Physics

Leem, Y.A., FSU, Physics

Rhee, S.J., Univ. of Illinois, Urbana-Champaign, Materials Research

Sung, M.G., SNU, Physics

Moon, I.C., SNU, Physics

GaAs/Al_{0.5}G_{0.5}As quantum wire arrays (QWA) were prepared by molecular beam epitaxy. The method used for the growth

of QWA is the tilted superlattice (TSL) method with migration enhanced epitaxy. The details of the growth procedure and TSL were described elsewhere.¹

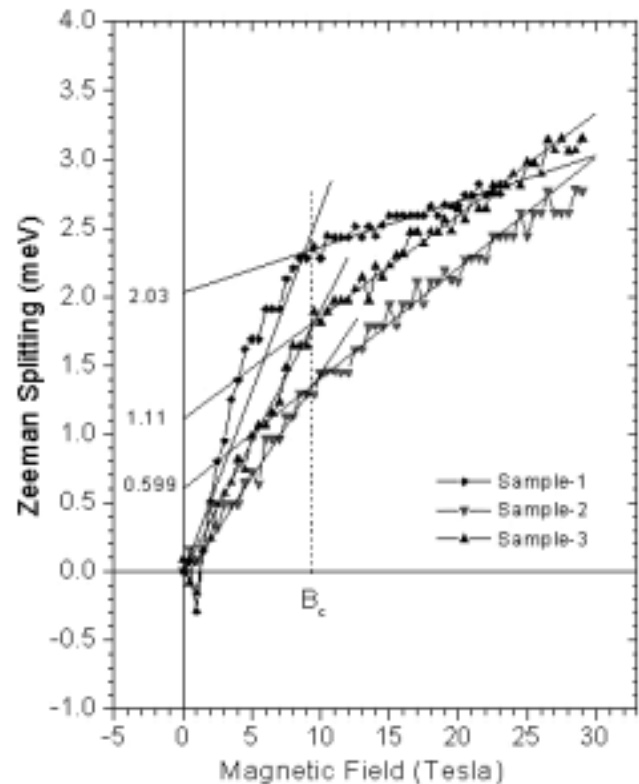


Figure 1. Zeeman spectra for the samples 1, 2, and 3.

Zeeman splittings in the radiative recombination of electron and heavy-hole excitons were obtained by polarization-dependent photoluminescence (PL). A strong magnetic field up to 30 T at the sample temperature of 4 K was applied in the direction perpendicular to the sample surface, which is a Faraday configuration. An external magnetic field (B_a) acts as a non-destructive perturbation to the exciton Hamiltonian and gives the effects of diamagnetic energy shift and Zeeman splitting. According to the selection rule, recombination luminescence has two opposite circular polarizations. By using the combination of circular polarizer and linear polarizer with the change of magnetic field direction, we can get PL of two different spin states. The Zeeman splitting energy data were obtained from the difference between these two.

As can be seen in Figure 1, Zeeman splitting abruptly changes its slope at some critical magnetic field, $B_a = B_c$. B_c is the point where the cyclotron radius of conduction electrons becomes equal to the wire width. Zeeman splitting energy (E_z) can be expressed in two regions of low and high magnetic field, as follows.

$$\begin{aligned} E_z &= g\mu_B B_a & (B_a < B_c) \\ E_z &= g'\mu_B B_a + E_0 & (B_a > B_c) \end{aligned}$$

Here, g and g' are effective g -factors, μ_B is the Bohr magneton, and E_0 is the zero-field splitting energy obtained from the extrapolation of Zeeman splitting at $B_a > B_c$ to $B_a = 0$.

The two equations must have continuity at $B_a = B_c$, and we can get the relation between g and g' , which is $g = g' + E_0/\mu_B B_c$. The g values obtained from this equation and from the slope of the data show almost the same value within the limit of error (see Table 1). The change of g factor in the two regions and the zero-field splitting can be explained by the quantization of electron orbits and spin-orbit interaction.

Table 1

	Sample-1	Sample-2	Sample-3
g	4.26	3.25	2.42
$g' + E_0/\mu_B B_c$	4.46	3.37	2.32

¹ Kim, D.H., *et al.*, Inst. Phys. Conf. Ser., **162**, 403 (1999).

Theoretical Study of Charge Density Wave Ordering in Partially Filled High Landau Levels

Yang, K., NHMFL/FSU, Physics

Rezayi, E.H., California State Univ., Physics

Haldane, F.D.M., Princeton Univ., Physics

Recently there is considerable interest in the behavior of a two-dimensional (2D) electron gas subject to a strong perpendicular magnetic field, when a high Landau level (with Landau level index $N=2$) is partially filled by electrons. This is inspired by the recent experimental finding of strong anisotropy in the longitudinal resistivity of the system when the highest Landau level occupied by electrons is half-filled.¹ Previously a Hartree-Fock study² suggests that when close to half filling, the electrons in the partially filled Landau level form one-dimensional (1D) charge density waves (CDW) (also called stripes); it is believed the anisotropy of the stripes is the origin of the anisotropy of the transport properties near such filling factors. The Hartree-Fock theory also predicts that sufficiently far away from half filling, these electrons form clusters or bubbles, while these bubbles form a triangular lattice; the ground state is thus a 2D CDW.

Motivated by these developments, we have been studying partially filled high Landau levels numerically using exact diagonalization of finite size systems. In these studies, we diagonalize the Hamiltonian of finite size systems with electrons occupying a partially filled Landau level, neglecting the mixing of different Landau levels. Typically we study systems containing 6 to 12 electrons. Such numerical studies played a crucial role in the understanding of the fractional quantum Hall effect when the lowest Landau level is partially filled. In our current study, we use the exact spectra and eigenstates generated by the exact diagonalization to calculate various correlation and response functions. We first studied the most interesting case of half-filled high Landau levels. Our results strongly suggest that 1D CDW (stripes) are formed in the

ground state,³ as indicated by the following findings: (a) We find the density response function $\chi(\mathbf{q})$ is sharply peaked at a one-dimensional array of wave vectors \mathbf{q}_n . (b) The ground state density-density correlation function is also peaked at these wave vectors. (c) The ground state wave functions have large overlaps with the stripe-based Hartree-Fock wave functions. (d) There exist a manifold of low-energy excited states that are nearly degenerate with the ground state; the degeneracy and quantum numbers of this ground state manifold are consistent with formation of stripes. The periodicity of the stripes determined from these studies agrees well with the predictions of the Hartree-Fock theory.

Currently we are studying the behavior of these systems away from half filling. We have found evidence that strongly suggests the formation of 2D instead of 1D CDW, when the filling factor is below 0.4. Specifically, we find that the positions of peaks of $\chi(\mathbf{q})$ form a 2D instead of 1D array in wave vector space. Other properties, like the degeneracy and quantum numbers of the ground state manifold, also suggest formation of 2D CDW. Currently we are continuing this work to pin down the position of the phase boundary separating the 1D and 2D CDWs.

¹ Lilly, M.P., *et al.*, Phys. Rev. Lett., **82**, 394 (1999); Du, R.R. *et al.*, Solid State Commun., **109**, 389 (1999).

² Fogler, M.M., *et al.*, Phys. Rev. B, **54**, 1853 (1996).

³ Rezayi, E.H., *et al.*, Phys. Rev. Lett., **83**, 1219 (1999).

Geometric Resonances of Composite Fermions in Microwave Conductivity Measurement

Ye, P.D., NHMFL/Princeton Univ., Electrical Eng.

Engel, L.W., NHMFL

Tsui, D.C., Princeton Univ., Electrical Eng.

Simmons, J.A., Sandia National Laboratories

Wendt, J.R., Sandia National Laboratories

Vawter, G.A., Sandia National Laboratories

Reno, J.R., Sandia National Laboratories

We have studied microwave conductivity, $\text{Re}(\sigma_{xx})$, of a high mobility two-dimensional electron system (2DES), patterned with an array of antidots, for frequency between 0.05 and 20 GHz in high magnetic fields. Antidot arrays of period $a=500$ nm or $1 \mu\text{m}$, and various etched depths, were fabricated by electron-beam lithography and dry etching in the slots of planar microwave transmission lines. We calculate $\text{Re}(\sigma_{xx})$ from the measured attenuation of the transmission line. At low magnetic fields, geometric resonance peaks of electrons are seen in both AC and DC transport.

Figure 1 shows $\text{Re}(\sigma_{xx})$ vs. B at high magnetic fields and microwave frequency of 2 GHz. We identify the asymmetric two-peak feature around filling factor $\nu=1/2$ as the resolved geometric resonance of composite Fermions.¹ The magnetic

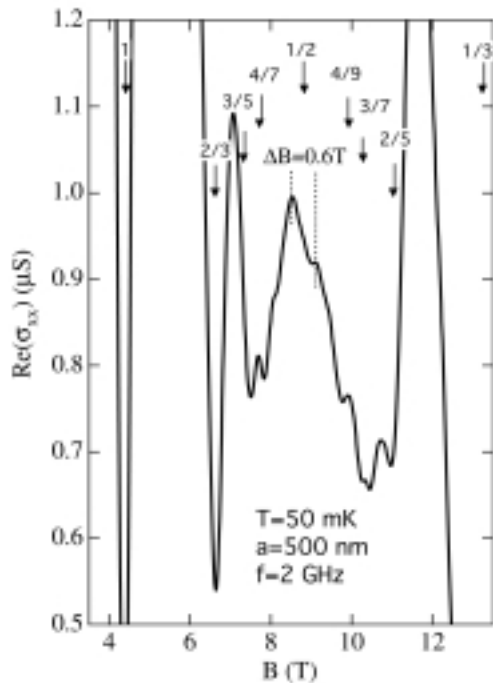


Figure 1. Real part of 2 GHz diagonal conductivity vs. magnetic field of an array of antidots with the period of 500 nm at $T=50$ mK. The two asymmetric geometric resonance peaks sitting around $\nu=1/2$ resemble features seen earlier in DC transport.¹

field distance between two resonance peaks is 0.6 T, in good agreement with the expected value for the commensurability relation $2R_C=a$ for fully polarized composite Fermions, where R_C is the cyclotron radius of composite Fermions. The commensurability resonance vanishes when the microwave frequency is beyond 5 GHz, possibly providing a hint concerning the effective mass of composite Fermions.

¹ Kang, W., *et al.*, Phys. Rev. Lett., 71, 3850 (1993).

Microwave Photoresistance in an Array of Antidots **IHRP**

Ye, P.D., NHMFL/Princeton Univ., Electrical Eng.
 Engel, L.W., NHMFL
 Tsui, D.C., Princeton Univ., Electrical Eng.
 Simmons, J.A., Sandia National Laboratories
 Wendt, J.R., Sandia National Laboratories
 Vawter, G.A., Sandia National Laboratories
 Reno, J.R., Sandia National Laboratories

We have studied microwave photoresistance of a high mobility two-dimensional electron gas (2DEG), patterned with an array of antidots, for microwave frequency, f , between 0.05 and 40 GHz, in low magnetic fields. The antidots, defined by electron beam lithography and dry etching, had 50 nm diameter and were 50 nm deep. The antidot array had 500 nm period, and was placed in the slots of a planar microwave transmission line that was used to apply a microwave field to the antidot array.

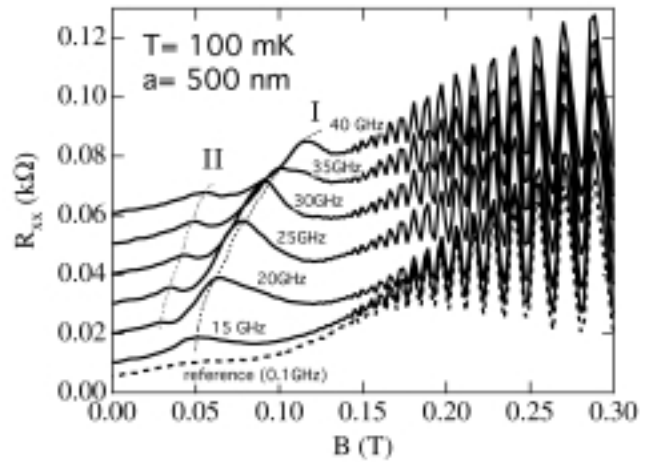


Figure 1. DC magnetoresistance with antidots exposed to a microwave field at a temperature of 100 mK. The traces (from top to bottom) are taken subsequently from $f=40$ GHz to 15 GHz with a step of 5 GHz and shifted for clarity. The oscillatory features in magnetoresistance above $B=0.12$ T are SdH oscillations. The dashed lines connecting the peaks are guides for the eye.

In microwave photoresistance, we observe oscillatory features with still unclear origins. Figure 1 shows DC diagonal resistance vs. B , for several fixed microwave frequencies applied to the antidot array. The higher B peak (marked I in the figure) occurs at $B=0.12$ T for the 40 GHz trace and shifts to lower fields on reducing the microwave frequency, reaching $B=0.05$ T for 15 GHz trace. The lower B peak (II in the figure) similarly shifts to lower fields and finally disappears when the microwave frequency is lower than 20 GHz. The B positions of peaks (I) are around 20% higher than the expected ones for cyclotron absorption, possibly because of the mixing of cyclotron resonance and plasmon modes in this two-dimensional modulated system, and peaks (II) appear near half¹ of the cyclotron resonance B . This broadband microwave photoresistance technique offers a unique approach to investigate the dynamic response of 2DEG in mK temperatures and high magnetic fields, filling the frequency gap between the conventional DC transport and far infrared (FIR) spectroscopy.

¹ Zudov, M.A., *et al.*, cond-mat/9711149.

Sub-GHz Microwave Resonance of Extremely Clean Two-Dimensional Electron System at $\nu < 1/5$ **IHRP**

Ye, P.D., NHMFL/Princeton Univ., Electrical Eng.
 Engel, L.W., NHMFL
 Tsui, D.C., Princeton Univ., Electrical Eng.
 Pfeiffer, L.N., Bell Labs, Lucent Technologies
 West, K.W., Bell Labs, Lucent Technologies

At high enough magnetic fields, 2D systems of carriers become insulators, which at low temperatures and for systems with sufficiently low disorder are probably some form of pinned

Wigner crystal (WC). Microwave resonances, found in low-filling insulating phases of both 2D electron¹ and 2D hole systems², are generally ascribed to a mode in which crystalline domains oscillate within the pinning potential. Since the mode is disorder-induced, it is of importance to test samples with various degrees of disorder; to our knowledge, the present sample is the cleanest for which the insulating phase resonance has been measured.^{1,2} The 2D system has mobility of $5 \cdot 10^6$ cm²/Vs and density of $6 \cdot 10^{10}$ /cm².

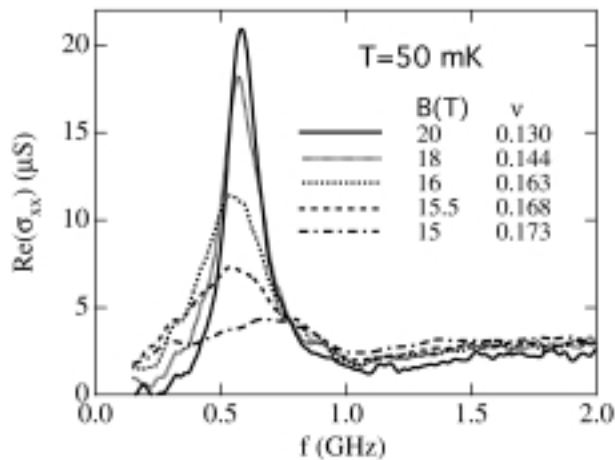


Figure 1. Real part of diagonal conductivity vs. frequency for several magnetic fields at $T=50$ mK.

Figure 1 shows the resonance as the real part of diagonal conductivity vs. frequency for several magnetic fields (highest $B=20$ T) at $T=50$ mK. For $\nu < 1/5$ ($B > 16$ T), a sharp resonance emerges and is at peak frequency of 0.58 GHz with a quality factor Q (peak frequency / full line width at half maximum) as large as 4 at $B=20$ T. As expected for a pinning mode, the resonance frequency is lower than those reported in References 1 and 2 for higher-disorder samples of similar carrier densities. The value of Q is similar to that seen for a p-type sample in Ref. 2, but has a high frequency tail like in Ref. 1. The “tail” of the resonance seen for frequency > 1 GHz resembles that seen for the higher-disorder sample of Ref. 1. The high frequency tail is hence likely to be a general feature of the resonance in n-type samples.

¹ Engel, L.W., *et al.*, Solid State Comm., **104**, 167 (1997)

² Li, C.C., *et al.*, Phys. Rev. Lett., **79**, 1353 (1997).

Magnetic Field Dependence of Cyclotron Resonance Linewidths in Modulation-Doped GaAs/AlGaAs and Si/SiGe Single Quantum Wells: A 2DEG with Long-Range Randomness

Yeo, T.M., State Univ. of New York at Buffalo, Physics

McCombe, B.D., SUNY at Buffalo, Physics

Ashkinadze, B.M., Technion-Israel Institute of Technology, Israel

Van Tol, J., NHMFL

Brunel, L.C., NHMFL

Pfeiffer, L., Lucent Technologies

Cyclotron resonance is a fundamental tool for studying the electronic properties of charge carriers in an external magnetic field, and there has been a great deal of work on cyclotron resonance in two dimensional electron gases (2DEGs)¹⁻³ over the past 25 years. A recent theoretical study, however, on CR linewidths in a 2DEG with long-range random potential fluctuations⁴ has predicted new and interesting behavior. These results show that with decreasing field the CR linewidth should linearly increase in the strong-field regime, reach a maximum at $R_c \sim d$ (R_c is the radius of the CR orbit and d is the correlation length of long-range random potential fluctuations), and then decrease in the intermediate-field regime. In this regime the CR linewidth is predicted to collapse to its classical value of τ^{-1} at $\omega_c \sim \omega_d$, where τ is the momentum relaxation time, ω_c is the CR frequency and ω_d is the frequency of the guiding center motion along the constant potential contours of the long-range random potential. In spite of extensive previous experimental work, a detailed systematic study over the very wide frequency and magnetic field ranges necessary to explore these predictions has not been carried out.

We have performed experimental studies of the CR linewidth over a very wide range of frequencies (1.2 cm⁻¹ to 142 cm⁻¹) in two high mobility, one-side modulation-doped GaAs/AlGaAs single quantum-well (SQW) samples (sample 1 has 3.2×10^{11} cm⁻² doping density and sample 2 has 6×10^{10} cm⁻² doping density) and one one-side modulation-doped Si/SiGe heterostructure (sample 3). Far-infrared laser (performed at SUNY at Buffalo) and microwave techniques (performed at NHMFL and Technion-Israel Institute of Technology) were used. Two different electron densities have been studied in detail for sample 1. The density was tuned by uniform above-barrier bandgap illumination. Figure 1 shows the results of CR linewidth analysis for three samples. The full widths at half maximum (FWHM) are plotted as a function of $1/(\omega_c \tau)$ to compare with the theoretical calculation. The critical values at which the CR linewidth is predicted to change are indicated by arrows ($1/(\omega_c \tau) < (W/E_F)^2$ is the strong-field regime and $1/(\omega_c \tau) > (W/E_F)^{4/3}$ is the weak-field regime. Here W is the rms amplitude of the random potential, and E_F is the Fermi

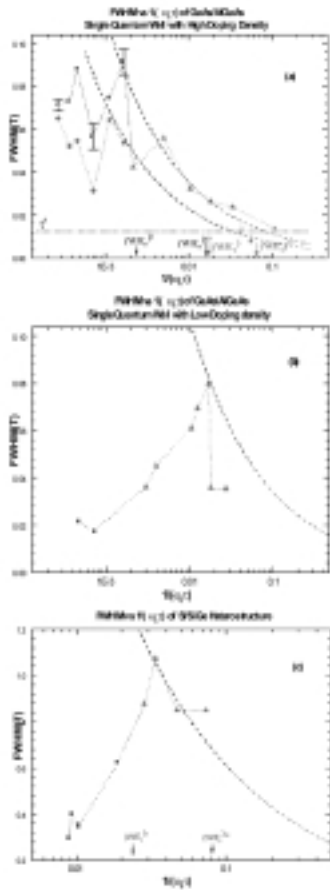


Figure 1. CR linewidth vs. $1/(\omega_c\tau)$ (a) sample 1, (b) sample 2, (c) sample 3. Square and diamond (with HeNe laser illumination) are for FIR data from SUNY at Buffalo, Triangle is for microwave data from NHMFL and circle is for microwave data from Israel. Dashed line is for Ando's calculation for CR linewidth in case of short range random potential. Arrows are for critical points of CR linewidth behaviors of long range random potential fluctuation.

energy). The dashed lines are calculated CR linewidths for the case of short range disorder.¹ For sample 1, we observe a large variation change of CR linewidth between the weak-field and strong-field regimes, and oscillations of the linewidth within the strong-field regime. The large change of CR linewidth from the strong field to the weak field regimes agree quite well with calculations for the case of short-range disorder.¹ For samples 2 and 3, we observe a linearly increasing linewidth in the strong-field regime, which, we believe, is consistent with the predicted behavior in this limit.⁴ Sample 2 shows an abrupt change of CR linewidth in the strong-field regime. To draw firm conclusions about the predicted collapse of the linewidth near $1/(\omega_c\tau) = (W/E_F)^{4/3}$ we need more detailed linewidth analysis. This analysis is ongoing.

¹ Ando, T., *J. Phys. Soc. Jpn.*, **38**, 989 (1975).

² Störmer, H.L., *et al.*, *Solid State Commun.* **29**, 703 (1979).

³ Watts, M., *et al.*, in *High Magnetic Field in Semiconductor Physics III*, edited by G. Landwehr (Springer-Verlag 1992), p. 581.

⁴ Fogler, M.M., *et al.*, *Phys. Rev. Lett.*, **80**, 4749 (1998).

Pressure Induced Quenching of Exciton Photoluminescence and Its Recovery by Magnetic Fields in CdTe/CdMnTe Quantum Wells

Yokoi, H., National Institute of Materials and Chemical Research, Japan

Tozer, S.W., NHMFL

Kim, Y., NHMFL/LANL

Wojtowicz, T., Polish Academy of Sciences, Institute of Physics

Karczewski, G., Polish Academy of Sciences, Institute of Physics

Kossut, J., Polish Academy of Sciences, Institute of Physics

Pressure effect on optical properties of Mn^{2+} d -electrons has been long investigated in diluted magnetic semiconductor $Cd_{1-x}Mn_xTe$. However, energy transfer between band electron and d -electron has not been studied in detail yet. We observed a photoluminescence (PL) signal from a 1.0 nm thick quantum well vanish by the application of pressures and restored by the application of magnetic fields in a $CdTe/Cd_{1-x}Mn_xTe$ ($x=0.4$) single quantum well structure. There is a possibility that these phenomena are due to the energy transfer mentioned above.

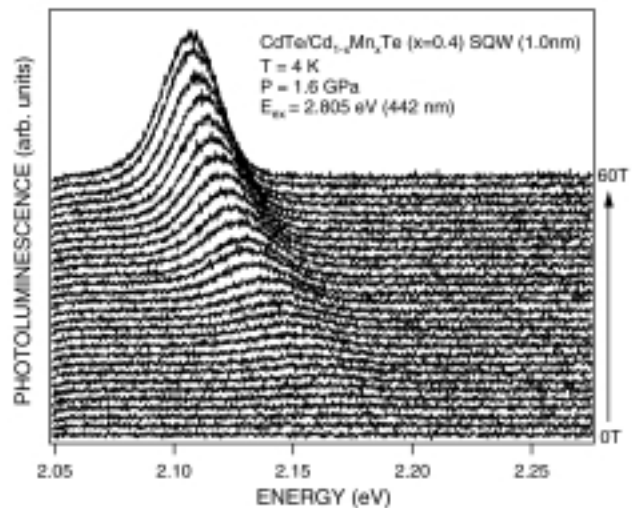


Figure 1. Field expansion of the PL spectrum between 2.05 and 2.275 eV every 2 T at 1.6 GPa and 4 K.

Magnetic fields were generated in a 60 T long pulsed magnet driven by a 1430 MW motor generator. A small diamond anvil cell with a plastic body was used in order to apply hydrostatic pressures to 2.1 GPa under pulsed magnetic fields. Excitation light from a He-Cd laser (442 nm) and luminescence signals from a sample were delivered through an optical fiber system.

An exciton PL signal from the 1.0 nm thick quantum well in the sample was observed at 2.05 eV in the condition of ambient pressure, 0 T and 4 K. With increasing the pressure, the PL peak position shifted to higher energy. The signal was observed up to 1.1 GPa and not above 1.6 GPa. At 1.6 GPa, the signal

was restored around 7 T, and became larger and shifted to lower energy with increasing the field. Figure 1 illustrates this phenomenon as a field expansion of the PL spectrum every 2 T. We interpret these phenomena in the following scenario: (1) The exciton PL vanishes when the band electron level becomes

higher than the *d*-electron level with increasing pressure and the energy transfer from the former to the latter is induced, (2) The PL is restored when the band electron level becomes lower than the *d*-electron level as a result of a Zeeman shift with increasing field.

MAGNETISM & MAGNETIC MATERIALS

Electrical Noise in $\text{La}_{2/3}\text{Sr}_{1/3}\text{MnO}_3$

Anane, A., FSU, Center for Materials Research and Technology (MARTECH)

Raquet, B., FSU, MARTECH and Institut National des Sciences Appliqués (INSA)-Toulouse-France

von Molnár, S., NHMFL/FSU, MARTECH

The current interest in the mixed valence perovskite manganites was originally fueled by the rediscovery of colossal magnetoresistance (CMR) in certain members of this group of materials.¹ The study of the physics of the manganites has, however, progressed far beyond CMR alone. Manganites have offered a fertile ground for the study of spin-charge interactions and transport-magnetism correlations. Furthermore, a multiphase description, where the insulator metal transition occurs via percolation has been proposed.² This picture of the coexistence of metallic and insulating phases, even in samples optimally doped to have the highest T_C , has recently been confirmed experimentally by Scanning Tunneling Microscopy (STM).³

Electrical noise results from transitions of switching entities called “fluctuators.” These transitions occur between states that have different conductivity. Studying the temperature and field dependence of the noise can provide insight into the electrical and magnetic nature of the fluctuators. Therefore, it is an effective tool for probing the dynamic behavior of an electrically inhomogeneous system, such as the manganites.

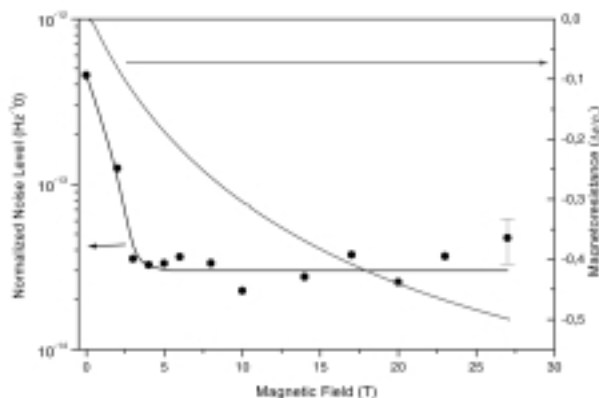


Figure 1. Magnetic field dependence of the power spectral density at 10Hz normalized to the applied voltage (left axis). Right axis represents the magnetoresistance vs. the magnetic field.

We have measured the $1/f$ noise resulting from the resistance fluctuations of a film of perovskite-type manganese oxide $\text{La}_{2/3}\text{Sr}_{1/3}\text{MnO}_3$ in the vicinity of the metal-insulator transition (300 K) in fields up to 27 T. Plotted in Figure 1 is the magnetic field dependence of the normalized noise level at 10 Hz (on the left axis) and the magnetoresistance (on the right axis). Whereas the magnetoresistance shows a monotonic decrease with no evidence of saturation, the noise level decreases sharply by roughly an order of magnitude between 0 and 3 T and seems to reach a baseline with no significant variations up to 27 T. These results show that the $1/f$ noise in $\text{La}_{2/3}\text{Sr}_{1/3}\text{MnO}_3$ does not probe the main conduction mechanism responsible for the nonsaturating magnetoresistance. We speculate that in this particular case the $1/f$ noise originates mainly from magnetic domain fluctuations that vanish when the sample is fully magnetized.

¹ Coey, J.M.D., *et al.*, *Adv. Phys.*, **48**, 167-293 (1998).

² Gor'kov, L.P., *et al.*, *J. Supercond.*, **12**, 243-246 (1999).

³ Fäth M, *et al.*, *Science*, **285**, 1540-1542 (1999).

High Field ESR Study of Polymeric Phases in $\text{Na}_2\text{Rb}_{1-x}\text{Cs}_x\text{C}_{60}$

Arcon, D., Univ. of Sussex, United Kingdom, Chemistry, Physics and Environmental Sciences, and J. Stefan Institute, Jamova, Slovenia

Prassides, K., Univ. of Sussex, United Kingdom, Chemistry, Physics and Environmental Sciences, and J. Stefan Institute, Jamova, Slovenia

Maniero, A.L., NHMFL

Brunel, L.-C., NHMFL

$\text{Na}_2\text{RbC}_{60}$ was shown to polymerise below about 250 K if the material is subjected to extremely slow cooling. Structural studies have confirmed the occurrence of polymerisation for the entire $\text{Na}_2\text{Rb}_{1-x}\text{Cs}_x\text{C}_{60}$ family at both ambient and elevated pressure. Both monomeric pc and monoclinic polymeric phases coexist below 250 K with the amount of the polymeric phase strongly depending on *x* as well as on cooling rate.

The polymerization of C_{60}^{3-} ions in $\text{Na}_2\text{RbC}_{60}$ is characterized by a different structural motif than that encountered in the extensively studied RbC_{60} polymer phase, involving a single C-C bridging bond. As a result, the C_{60} - C_{60} intrachain distance (~9.35 Å) in $\text{Na}_2\text{RbC}_{60}$ is longer than that in RbC_{60} (~9.11